

**Structure-Reactivity Correlation in selective colorimetric detection of cyanide
in solid, organic and aqueous phases using quinone based chemodosimeters**

R. Manivannan and Kuppanagounder P. Elango*

Supporting Information

Figure No.	Content	Page No.
S1	Color change of S1-S5 with various anions	5
S2	UV-Vis spectra of S2 with addition of CN ⁻ ion	6
S3	UV-Vis spectra of S3 with addition of CN ⁻ ion	7
S4	UV-Vis spectra of S4 with addition of CN ⁻ ion	8
S5	UV-Vis spectra of S5 with addition of CN ⁻ ion	9
S6	Correlation between Hammett's substituent constants (σ_p) and λ_{ICT} values	10
S7	Fluorescence emission spectra of S2 with addition of CN ⁻ ion	11
S8	Fluorescence emission spectra of S3 with addition of CN ⁻ ion	12
S9	Fluorescence emission spectra of S4 with addition of CN ⁻ ion	13
S10	Fluorescence emission spectra of S5 with addition of CN ⁻ ion	14
	Determination of binding constant (K)	15
S11	Benesi-Hildebrand plot of S1-CN⁻ complex	16
S12	Benesi-Hildebrand plot of S2-CN⁻ complex	17

S13	Benesi-Hildebrand plot of S3 -CN ⁻ complex	18
S14	Benesi-Hildebrand plot of S4 -CN ⁻ complex	19
S15	Benesi-Hildebrand plot of S5 -CN ⁻ complex	20
S16	Job's plot of S1 with CN ⁻ ion	21
S17	Detection limit plot of S1 -CN ⁻ complex	22
S18	Detection limit plot of S2 -CN ⁻ complex	23
S19	Detection limit plot of S3 -CN ⁻ complex	24
S20	Detection limit plot of S4 -CN ⁻ complex	25
S21	Detection limit plot of S5 -CN ⁻ complex	26
S22	¹ H NMR spectrum of S2 with addition of (a) 0 eqv. (b) 0.5 eqv. (c) 1.0 eqv. of TBACN in DMSO-d ₆	27
S23	¹ H NMR spectrum of S3 with addition of (a) 0 eqv. (b) 0.5 eqv. (c) 1.0 eqv. of TBACN in DMSO-d ₆	28
S24	¹ H NMR spectrum of S4 with addition of (a) 0 eqv. (b) 0.5 eqv. (c) 1.0 eqv. of TBACN in DMSO-d ₆ .	29
S25	¹ H NMR spectrum of S5 with addition of (a) 0 eqv. (b) 0.5 eqv. (c) 1.0 eqv. of TBACN in DMSO-d ₆	30
S26	¹ H NMR spectrum of (a) free S1 (b) S1 + 0.5 eqv. F ⁻ (c) S1 + (0.5 eqv. F ⁻) + 2 eqv. CN ⁻ (d) S1 + 1 eqv. CN ⁻	31
S27	¹³ C NMR spectrum of S5 with addition of TBACN in DMSO-d ₆	32
S28	Changes in redox properties of S2 upon addition of TBACN in ACN	33
S29	Changes in redox properties of S3 upon addition of TBACN in ACN	34
S30	Changes in redox properties of S4 upon addition of	35

	TBACN in ACN	
S31	Changes in redox properties of S5 upon addition of TBACN in ACN	36
S32	Optimized structure for sensors S1-S5 and its cyanide complex	37
S33	Molecular orbitals (HOMO–LUMO) of sensors S1-S5	38
S34	Molecular orbitals (HOMO –LUMO) of sensors– CN ⁻ complexes	39
Table S1	Energies (in eV) of the MOs in free sensors and in sensor- CN ⁻ ion complexes	40
S35	Color change of test strips upon dipping in solution of NaCN in deep well water.	41
S36	¹ H NMR spectrum of S1 in DMSO-d ₆	42
S37	¹ H- ¹ H COSY spectrum of S1 in DMSO-d ₆	43
S38	¹³ C NMR spectrum of S1 in DMSO-d ₆	44
S39	LCMS spectrum of S1	45
S40	¹ H NMR spectrum of S2 in DMSO-d ₆	46
S41	¹³ C NMR spectrum of S2 in DMSO-d ₆	47
S42	LCMS spectrum of S2	48
S43	¹ H NMR spectrum of S3 in DMSO-d ₆	49
S44	¹ H- ¹ H COSY spectrum of S3 in DMSO-d ₆	50
S45	¹³ C NMR spectrum of S3 in DMSO-d ₆	51
S46	LCMS spectrum of S3	52
S47	¹ H NMR spectrum of S4 in DMSO-d ₆	53
S48	¹ H- ¹ H COSY spectrum of S4 in DMSO-d ₆	54

S49	¹³ C NMR spectrum of S4 in DMSO-d ₆	55
S50	LCMS spectrum of S4	56
S51	¹ H NMR spectrum of S5 in DMSO-d ₆	57
S52	¹³ C NMR spectrum of S5 in DMSO-d ₆	58
S53	LCMS spectrum of S5	59
S54	¹ H NMR spectrum of S5-CN⁻ complex in DMSO-d ₆	60
S55	¹³ C NMR spectrum of S5-CN⁻ complex in DMSO-d ₆	61
S56	LCMS spectrum of S5-CN⁻ complex	62



Fig. S1. Color change of **S1-S5** (6.25×10^{-5} M) with various anions.

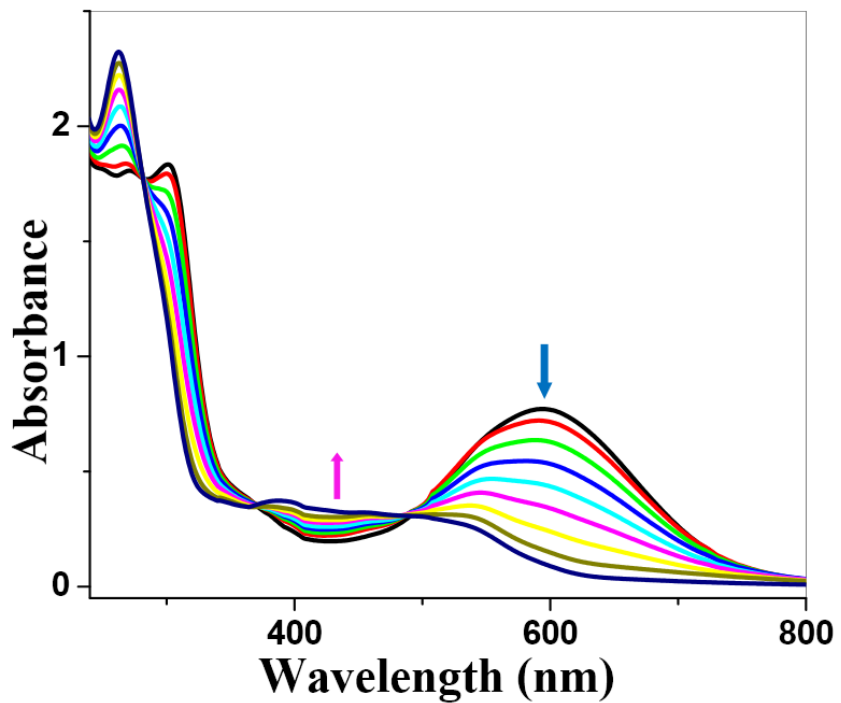


Fig. S2. UV-Vis spectra of **S2** (6.25×10^{-5} M) with incremental addition of TBACN (0- 6.25×10^{-6} M) in aq. HEPES buffer/ACN (8:2 v/v).

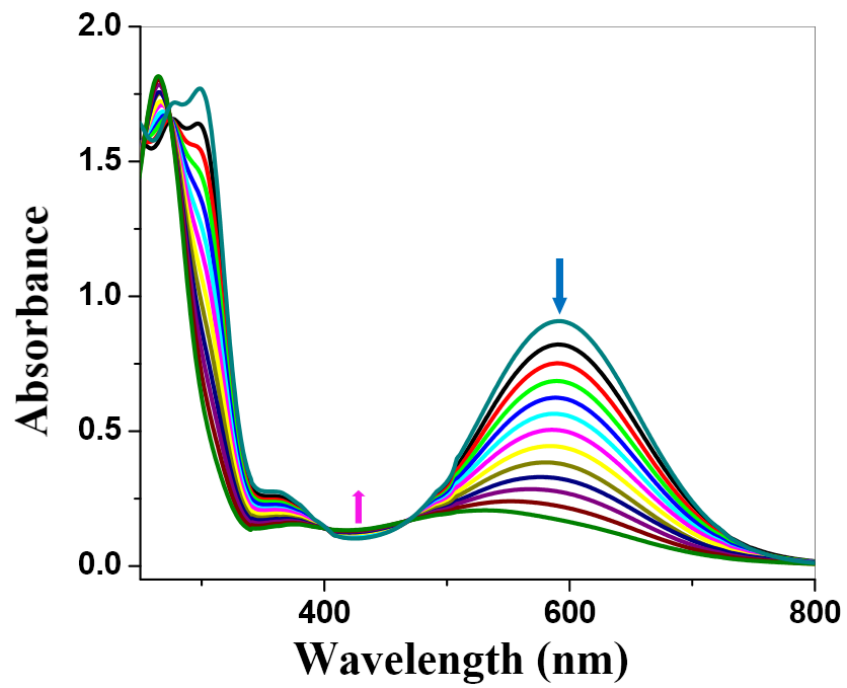


Fig. S3. UV-Vis spectra of **S3** (6.25×10^{-5} M) with incremental addition of TBACN ($0-6.25 \times 10^{-6}$ M) in aq. HEPES buffer/ACN (8:2 v/v).

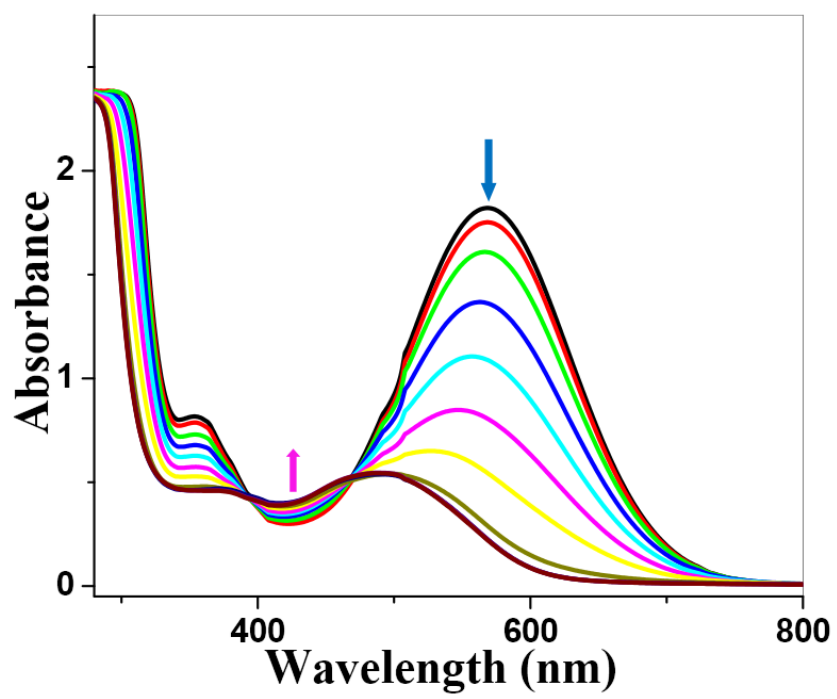


Fig. S4. UV-Vis spectra of **S4** (6.25×10^{-5} M) with incremental addition of TBACN ($0\text{--}6.25 \times 10^{-6}$ M) in aq. HEPES buffer/ACN (8:2 v/v).

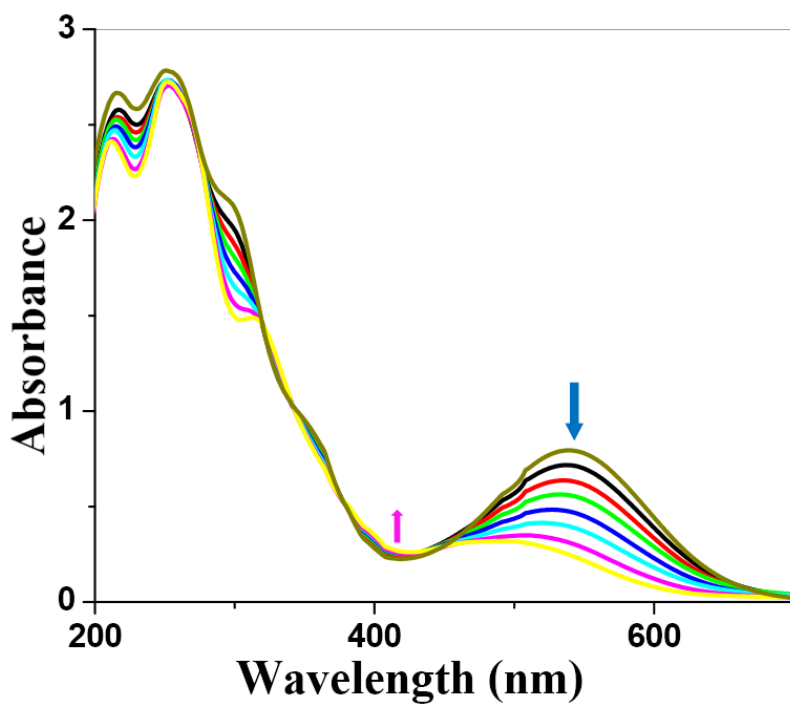


Fig. S5. UV-Vis spectra of **S5** (6.25×10^{-5} M) with incremental addition of TBACN ($0\text{--}6.25 \times 10^{-6}$ M) in aq. HEPES buffer/ACN (8:2 v/v).

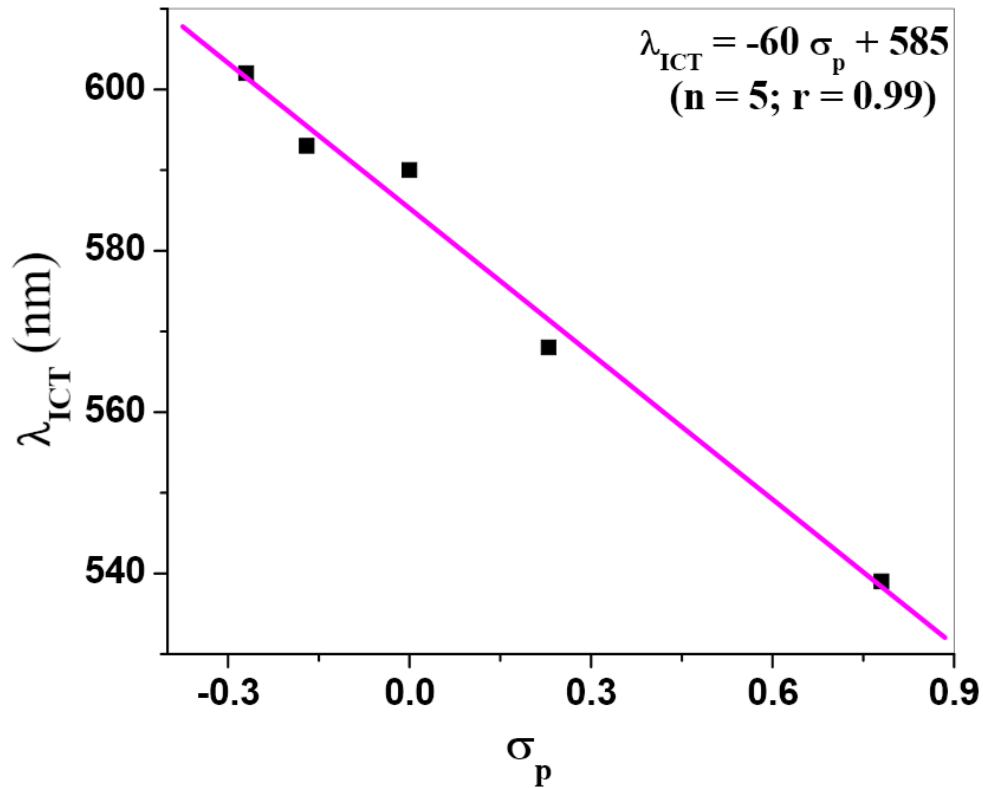


Fig. S6. Correlation between the λ_{ICT} and the Hammett's substituent constants (σ_p)

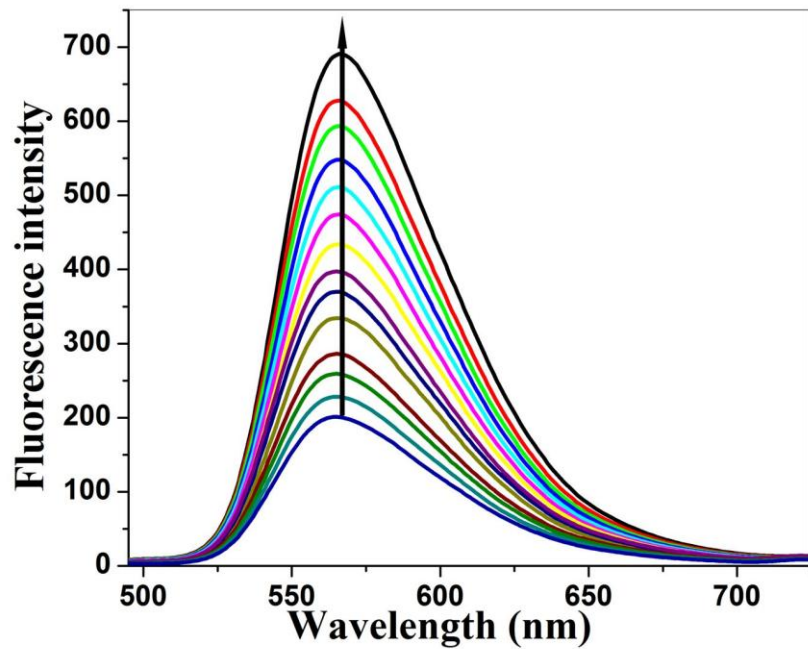


Fig. S7. Fluorescence spectra of **S2** (6.25×10^{-5} M) with incremental addition of TBACN (0- 6.25×10^{-6} M) in aq. HEPES buffer/ACN (8:2 v/v).

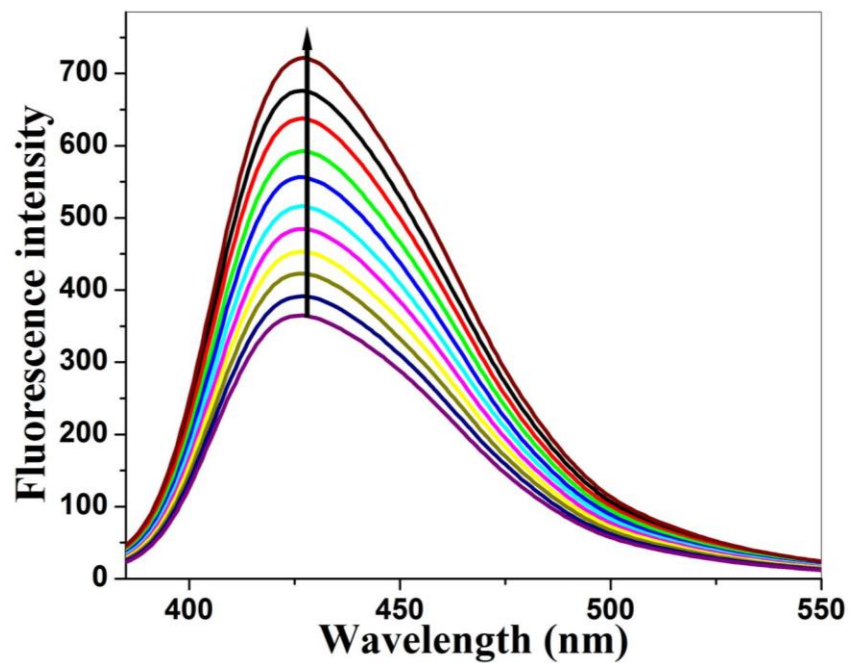


Fig. S8. Fluorescence spectra of **S3** (6.25×10^{-5} M) with incremental addition of TBACN (0- 6.25×10^{-6} M) in aq. HEPES buffer/ACN (8:2 v/v).

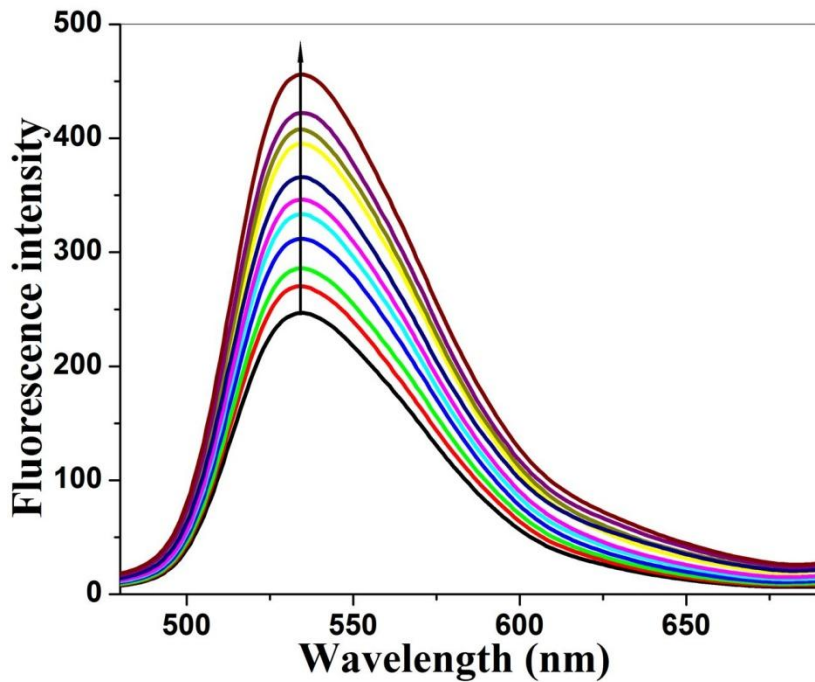


Fig. S9. Fluorescence spectra of **S4** (6.25×10^{-5} M) with incremental addition of TBACN (0- 6.25×10^{-6} M) in aq. HEPES buffer/ACN (8:2 v/v).

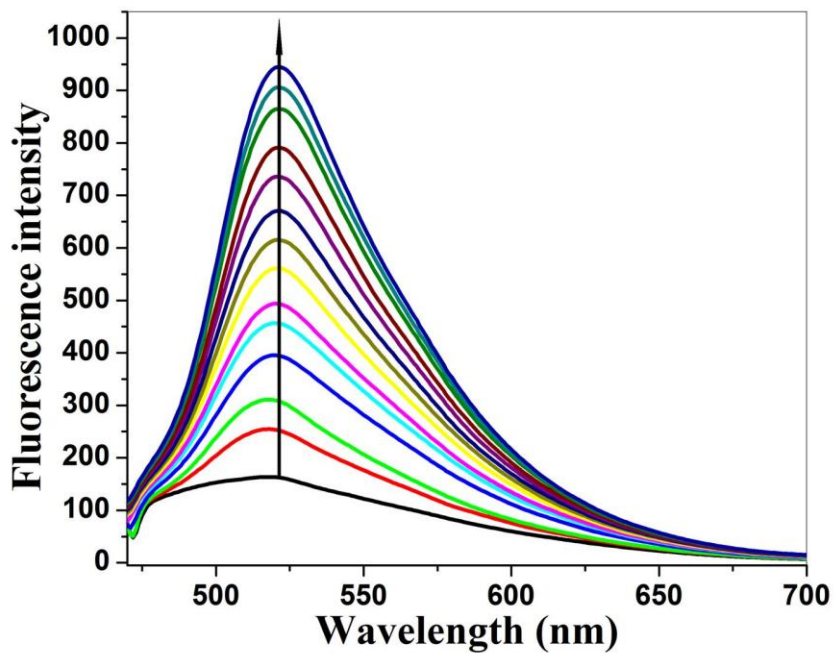


Fig. S10. Fluorescence spectra of **S5** (6.25×10^{-5} M) with incremental addition of TBACN (0- 6.25×10^{-6} M) in aq. HEPES buffer/ACN (8:2 v/v).

Determination of binding constant (K)

From the fluorescence enhancement data the binding constants for the sensors-cyanide complexes can be determined using the following Benesi-Hildebrand equation [37]:

$$(F_\infty - F_o) / (F_x - F_o) = 1/K [CN^-]$$

Where F_o , F_x and F_∞ are the fluorescence intensities of the sensor in the absence of cyanide ions, at given cyanide ion concentrations and at a concentration for complete interaction, respectively. In the present study in all the cases plots of $(F_\infty - F_o) / (F_x - F_o)$ versus $1/[CN^-]$ are linear ($r > 0.995$; Fig. S11-S15).

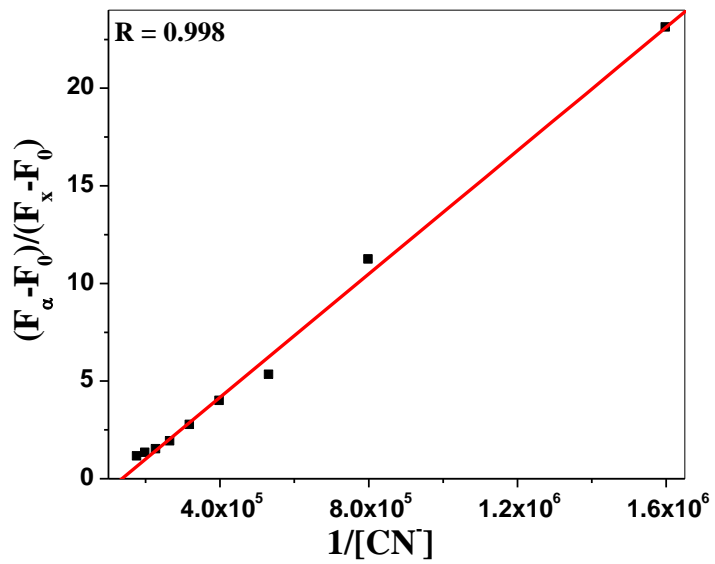


Fig. S11. Benesi-Hildebrand plot of **S1**-CN⁻ complex.

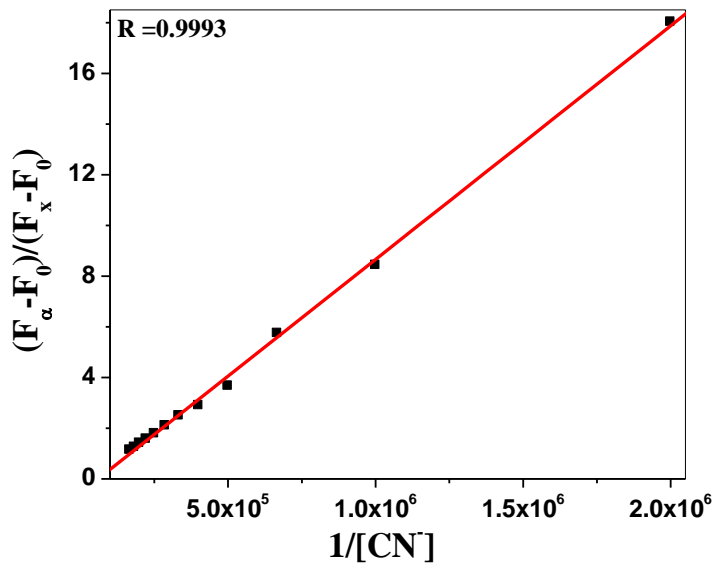


Fig. S12. Benesi-Hildebrand plot of S2-CN⁻ complex.

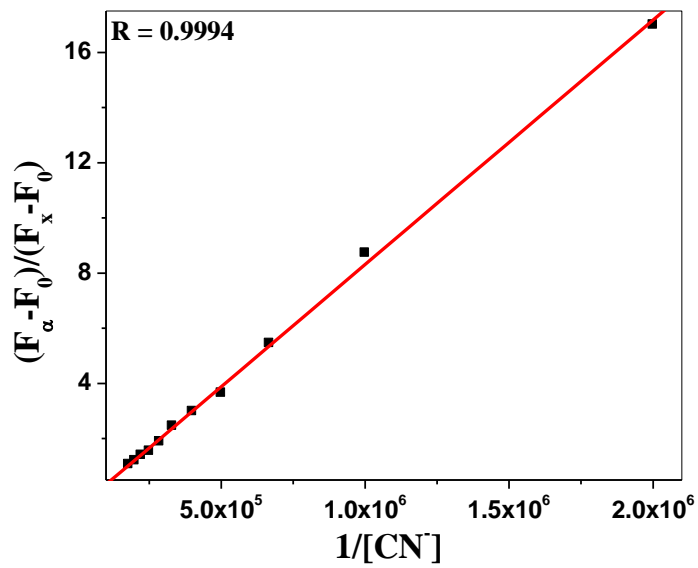


Fig. S13. Benesi-Hildebrand plot of S3-CN⁻ complex.

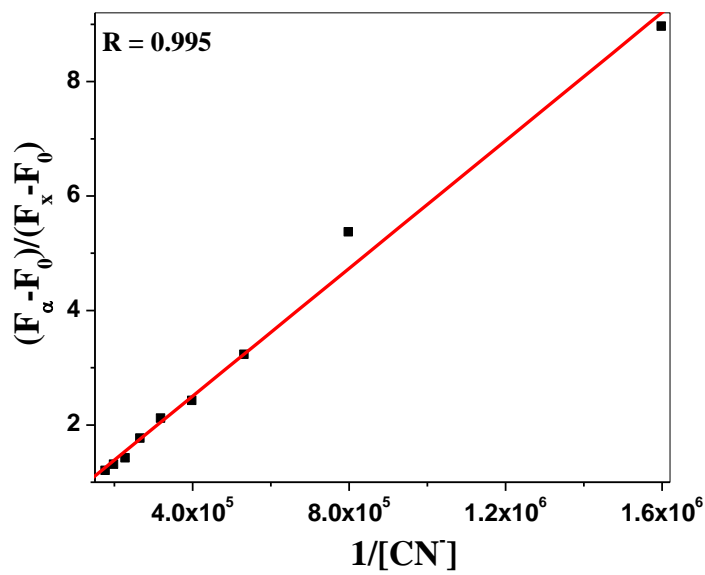


Fig. S14. Benesi-Hildebrand plot of S4-CN⁻ complex.

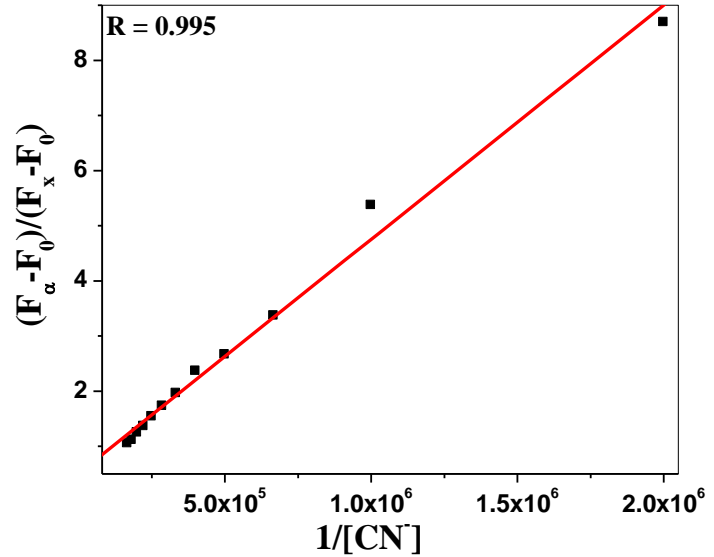


Fig. S15. Benesi-Hildebrand plot of S5-CN⁻ complex.

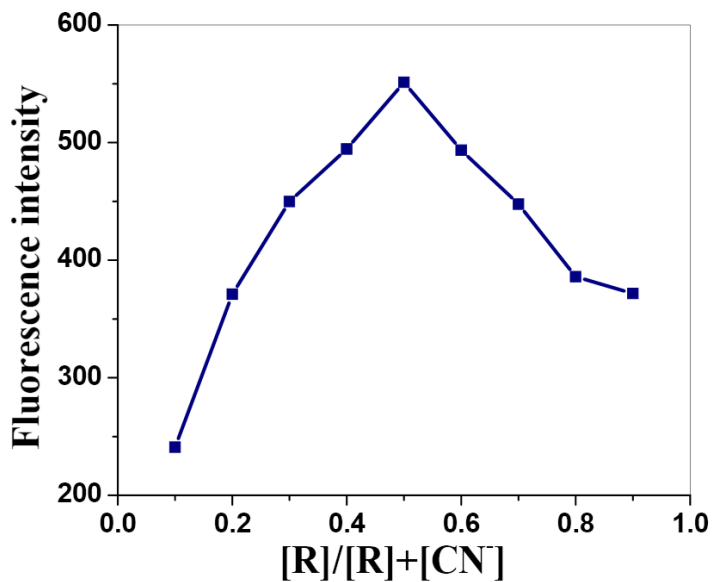


Fig. S16. Job's plot of **S1** with F^- and CN^- ion.

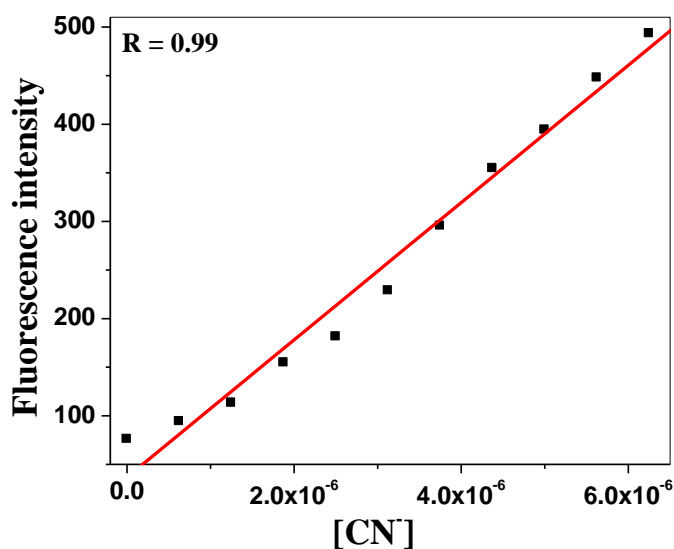


Fig. S17. Detection limit plot of **S1**- CN^- complex.

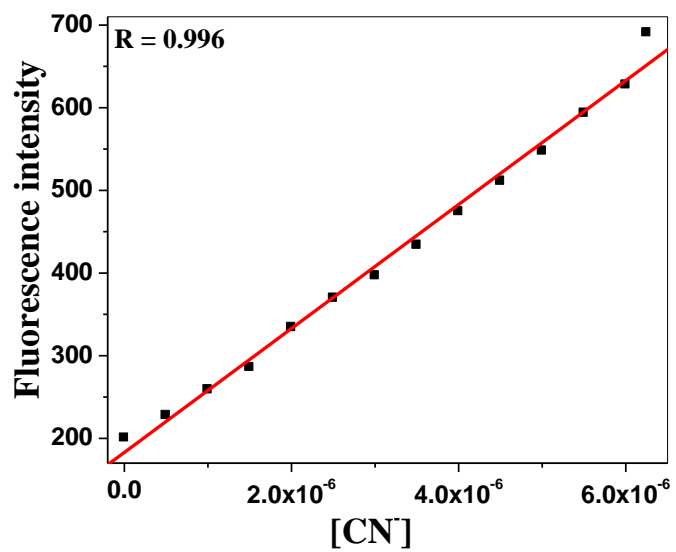


Fig. S18. Detection limit plot of S2-CN⁻ complex.

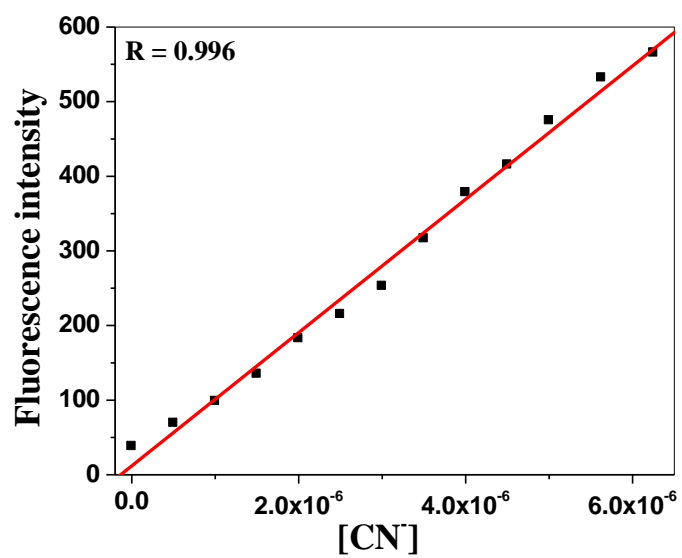


Fig. S19. Detection limit plot of S3-CN⁻ complex.

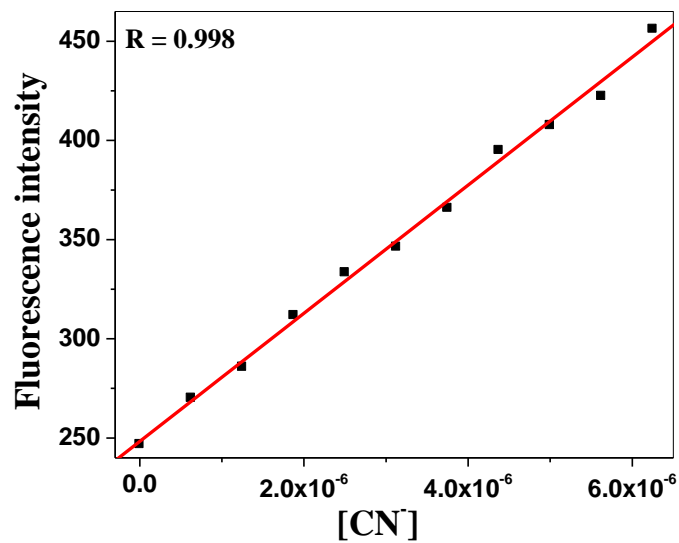


Fig. S20. Detection limit plot of S4-CN⁻ complex.

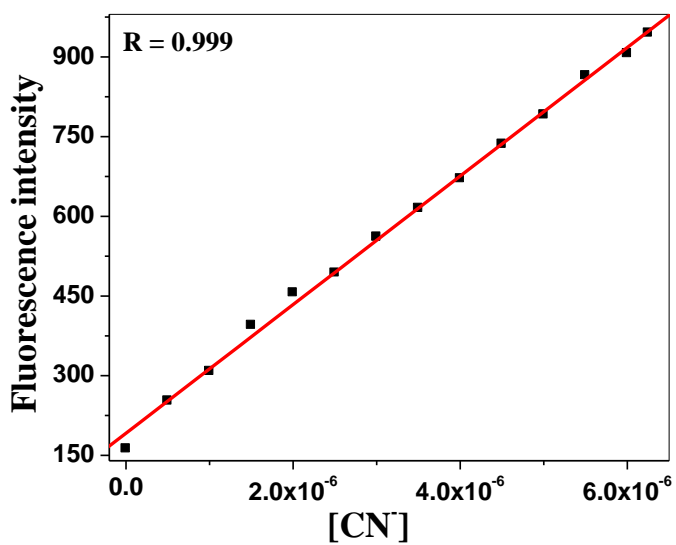


Fig. S21. Detection limit plot of S5-CN⁻ complex.

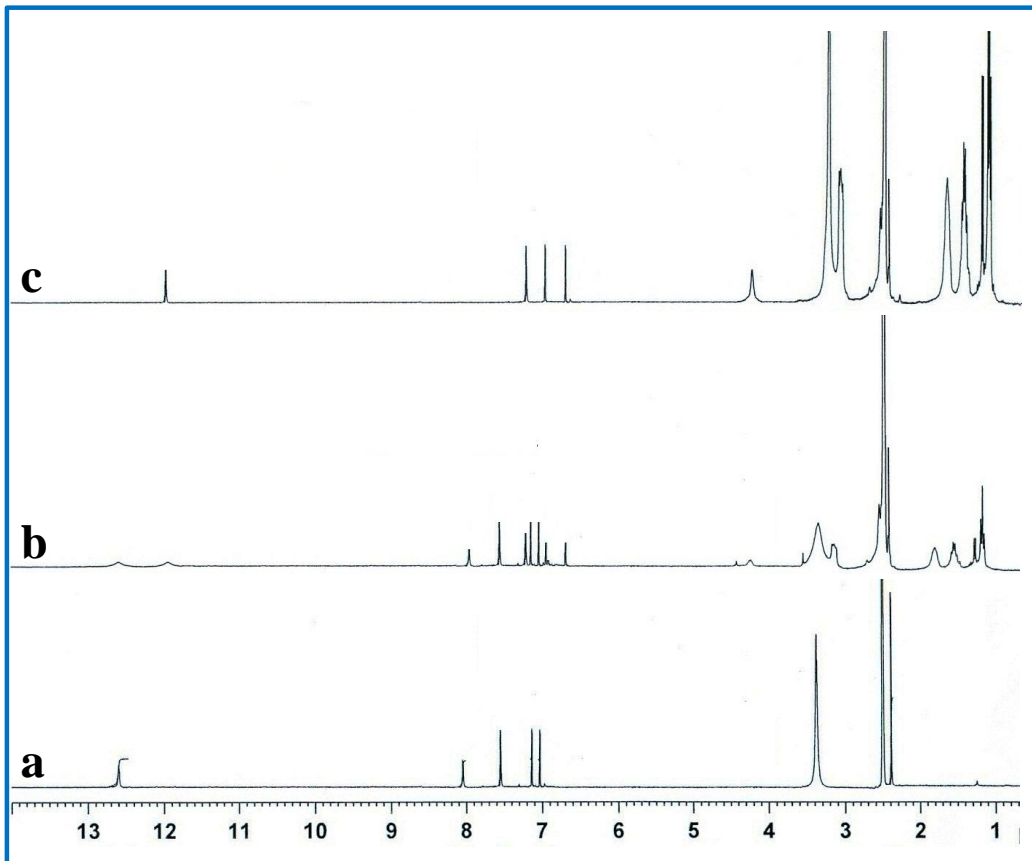


Fig. S22. ¹H NMR spectrum of S2 with addition of (a) 0 eqv. (b) 0.5 eqv. (c) 1.0 eqv. of TBACN in DMSO-d₆.

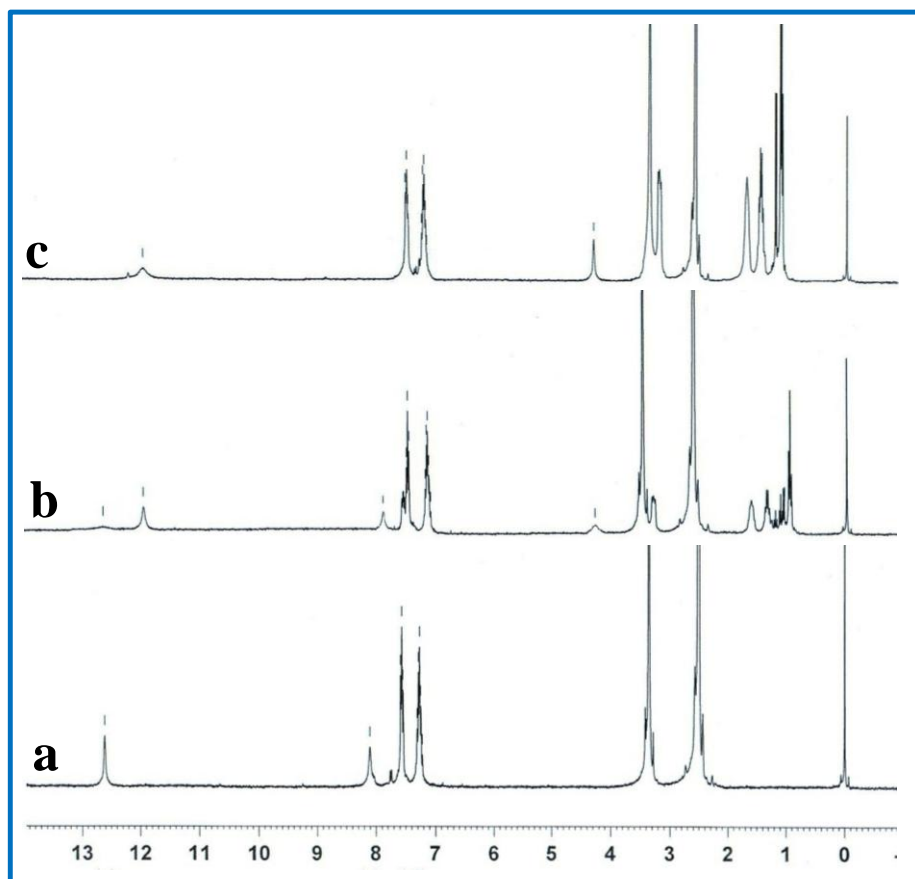


Fig. S23. ¹H NMR spectrum of S3 with addition of (a) 0 eqv. (b) 0.5 eqv. (c) 1.0 eqv. of TBACN in DMSO-d₆.

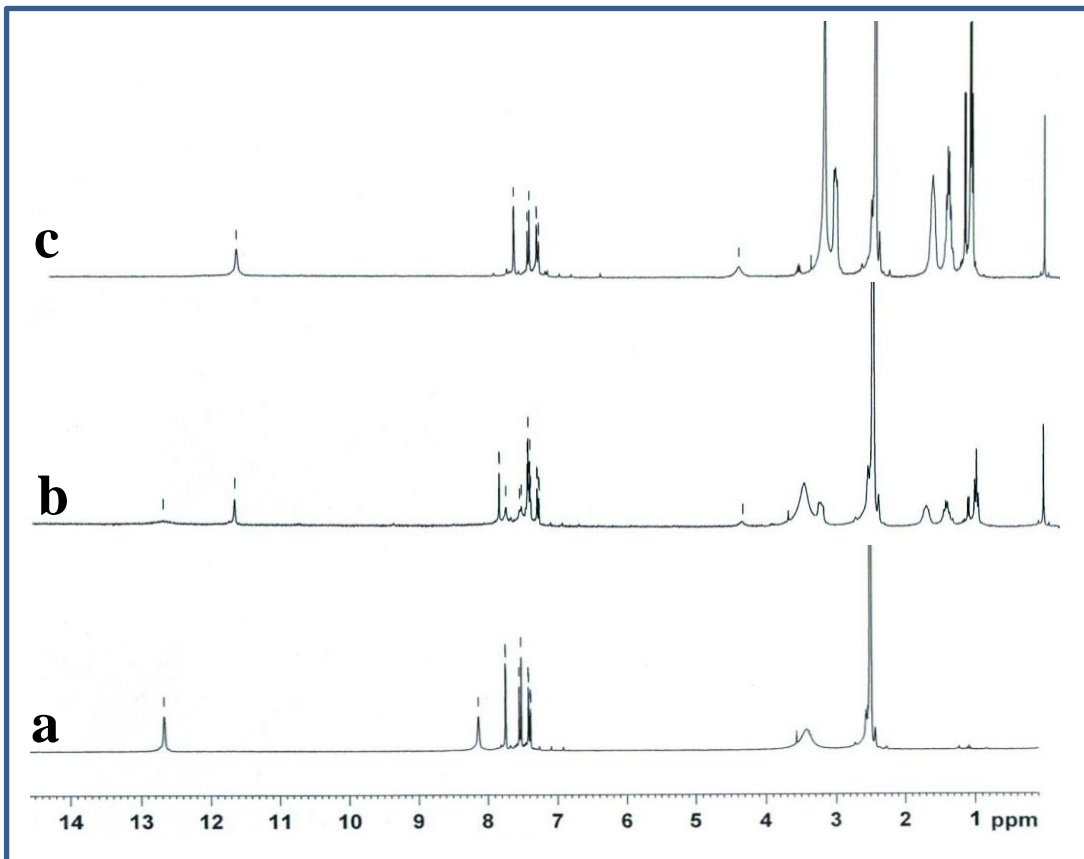


Fig. S24. ¹H NMR spectrum of **S4** with addition of (a) 0 equiv. (b) 0.5 equiv. (c) 1.0 equiv. of TBACN in DMSO-d₆.

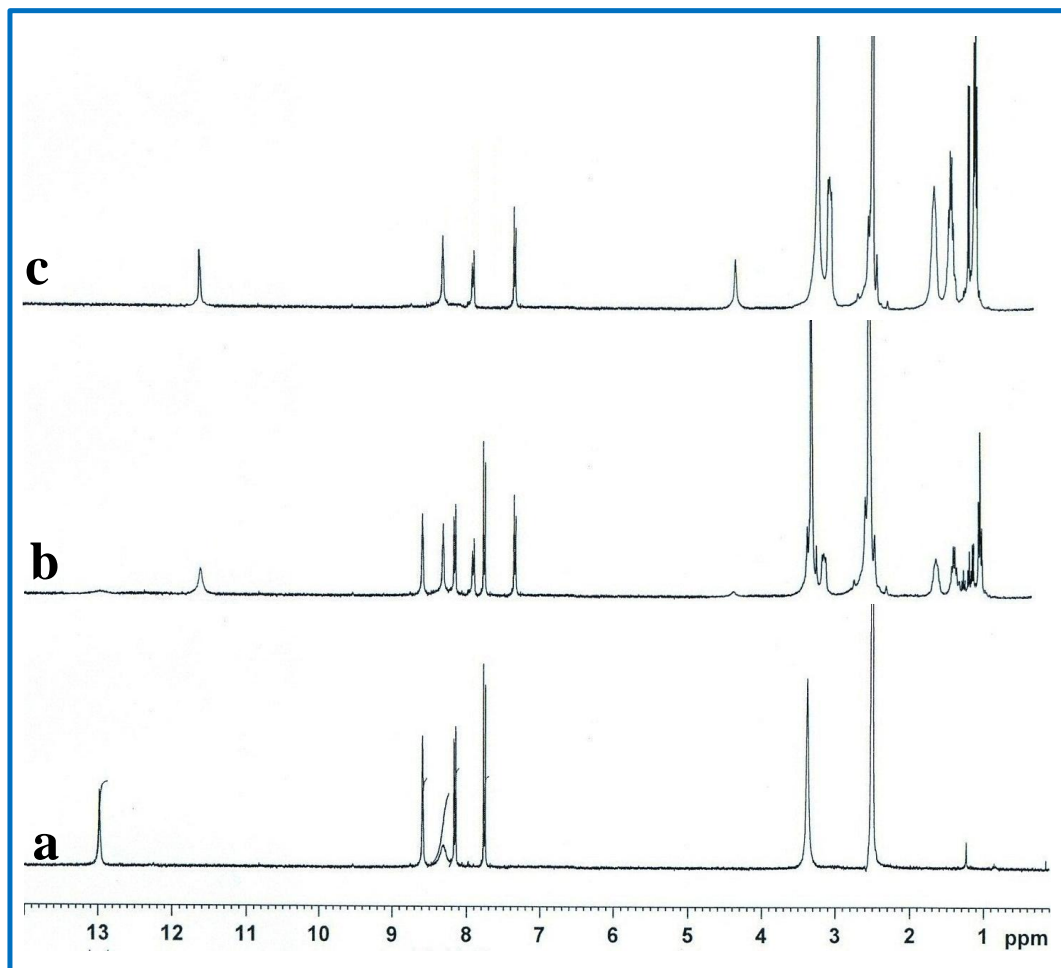


Fig. S25. ¹H NMR spectrum of S5 with addition of (a) 0 equiv. (b) 0.5 equiv. (c) 1.0 equiv. of TBACN in DMSO-d₆.

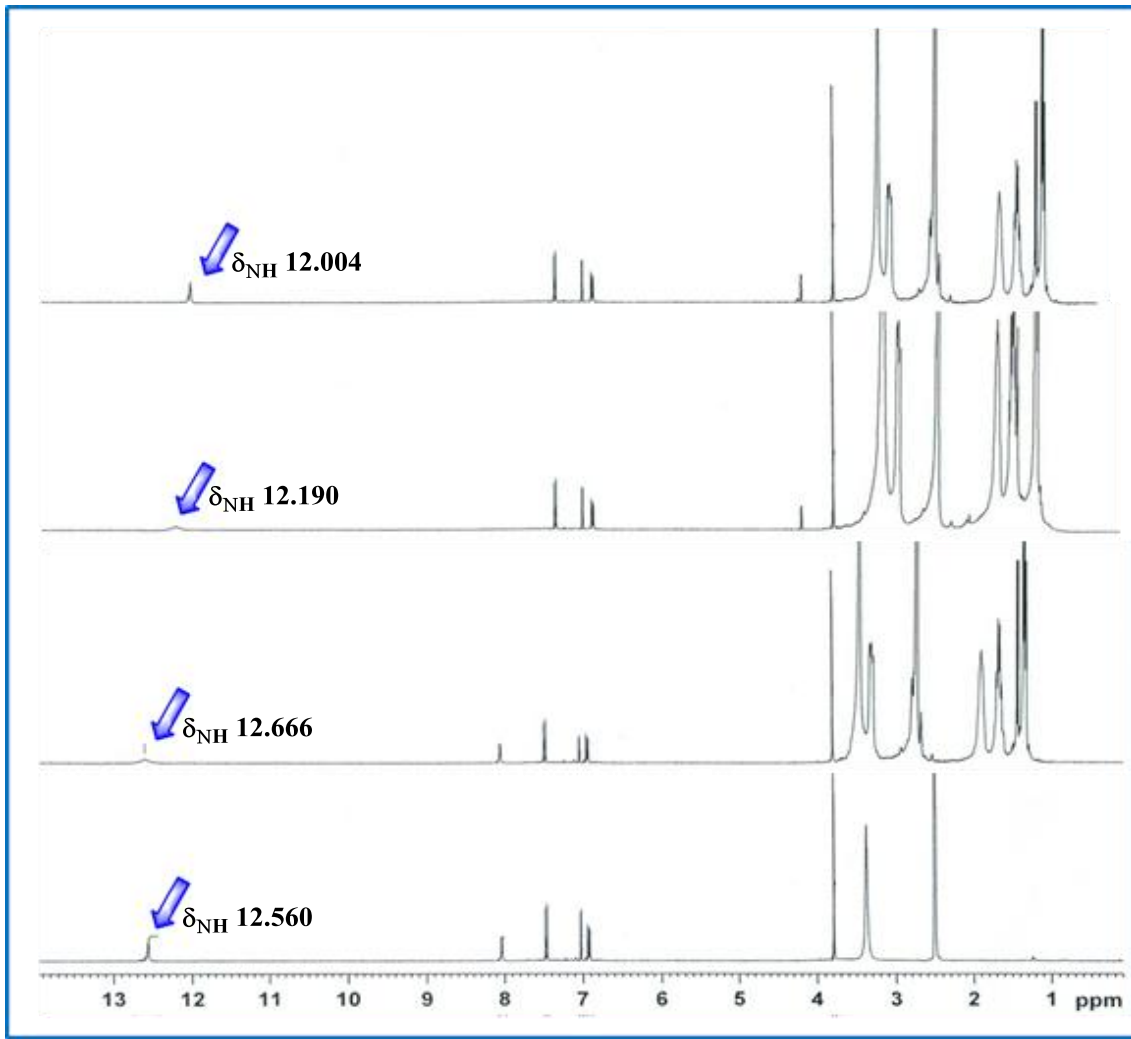


Fig. S26. ¹H NMR spectrum of (a) free **S1** (b) **S1** + 0.5 equiv. F⁻ (c) **S1** + (0.5 equiv. F⁻) + 2 equiv. CN⁻ (d) **S1** + 1 equiv. CN⁻.

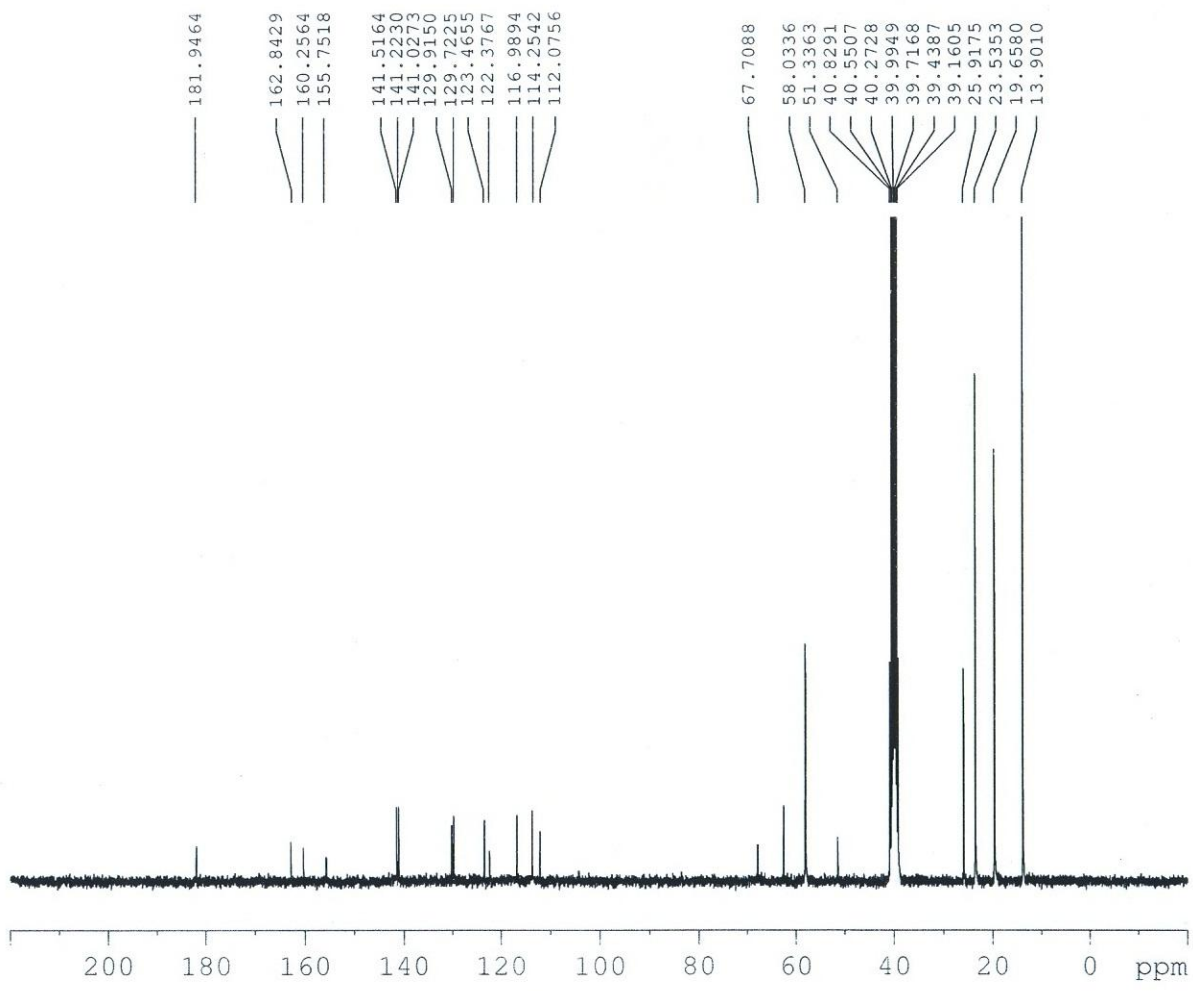


Fig. S27. ¹³C NMR spectrum of S5 with addition of TBACN in DMSO-d₆.

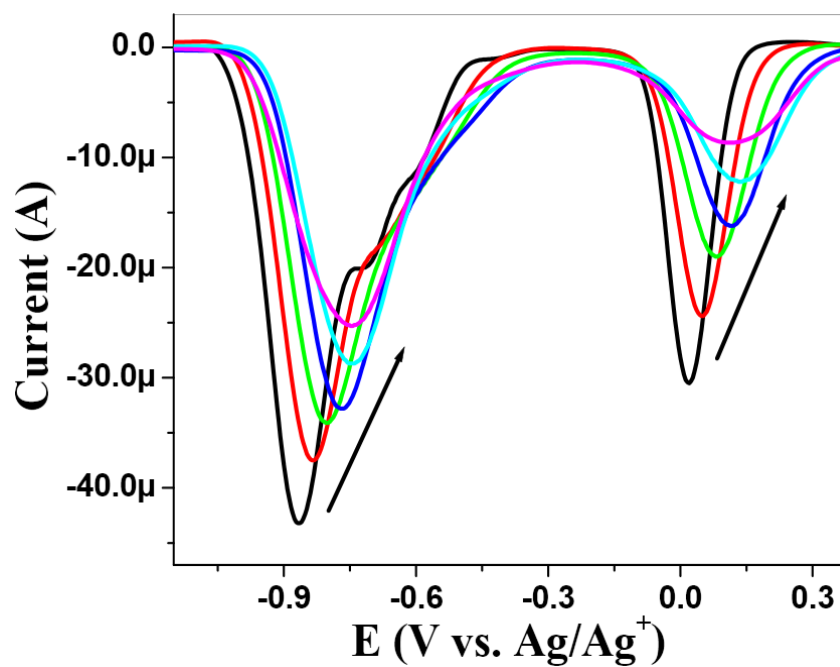


Fig. S28. Changes in redox properties of **S2** upon addition of TBACN in ACN.

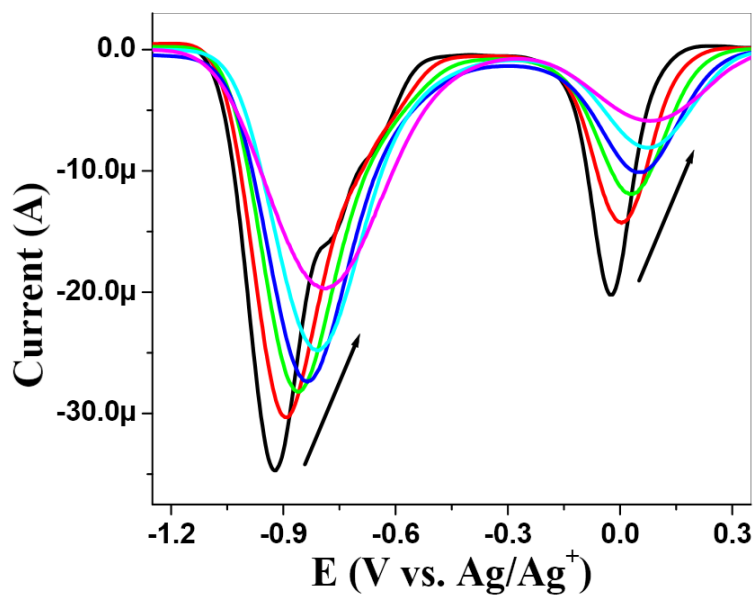


Fig. S29. Changes in redox properties of **S3** upon addition of TBACN in ACN.

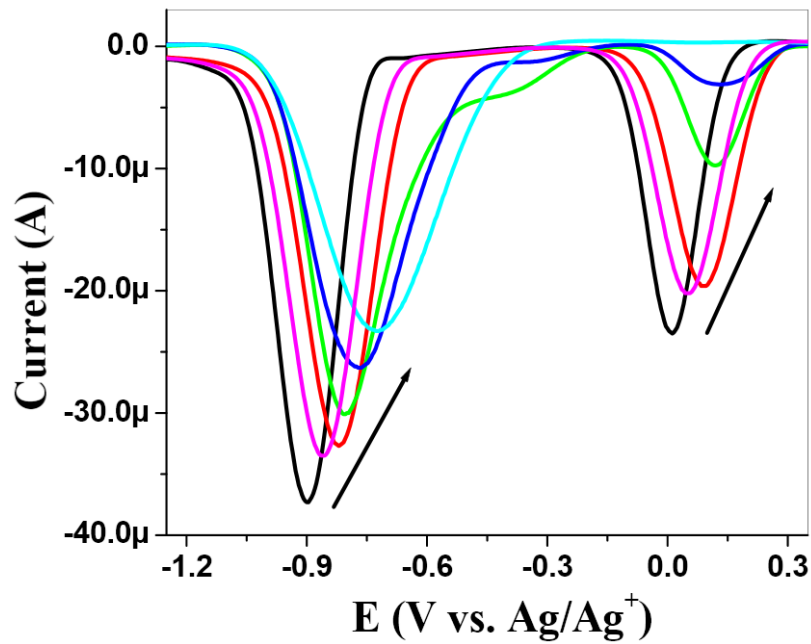


Fig. S30. Changes in redox properties of **S4** upon addition of TBACN in ACN.

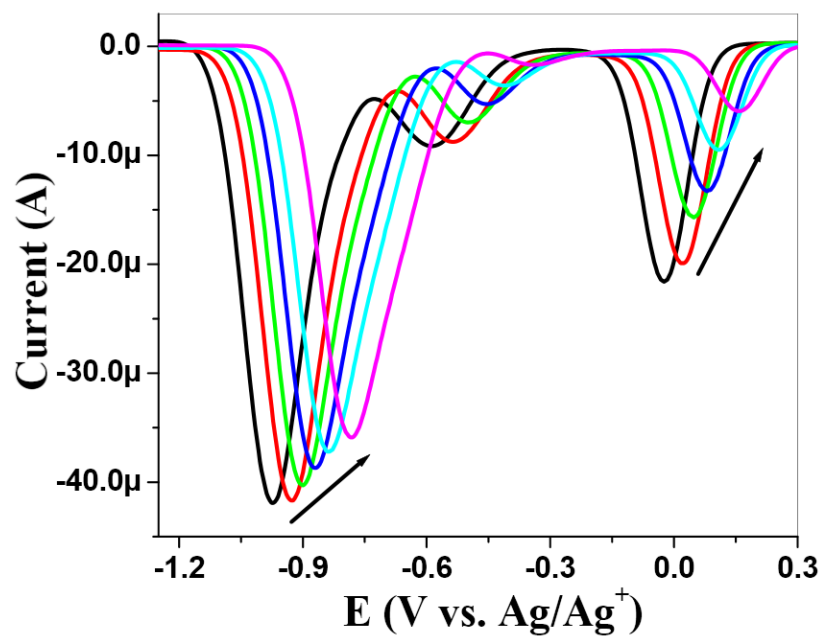


Fig. S31. Changes in redox properties of **S5** upon addition of TBACN in ACN.

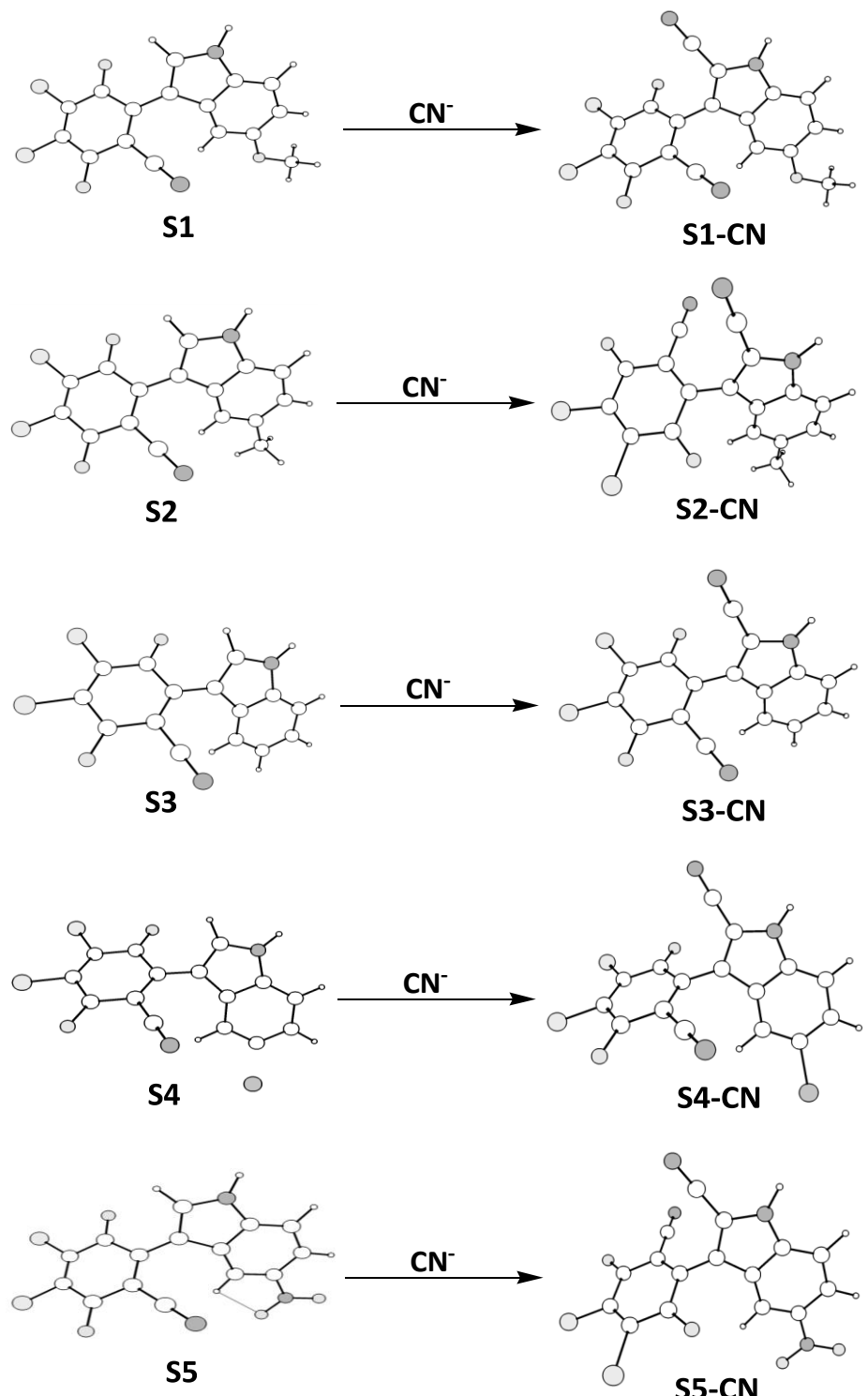


Fig. S32. Optimized structure for sensors **S1-S5** and its cyanide complex.

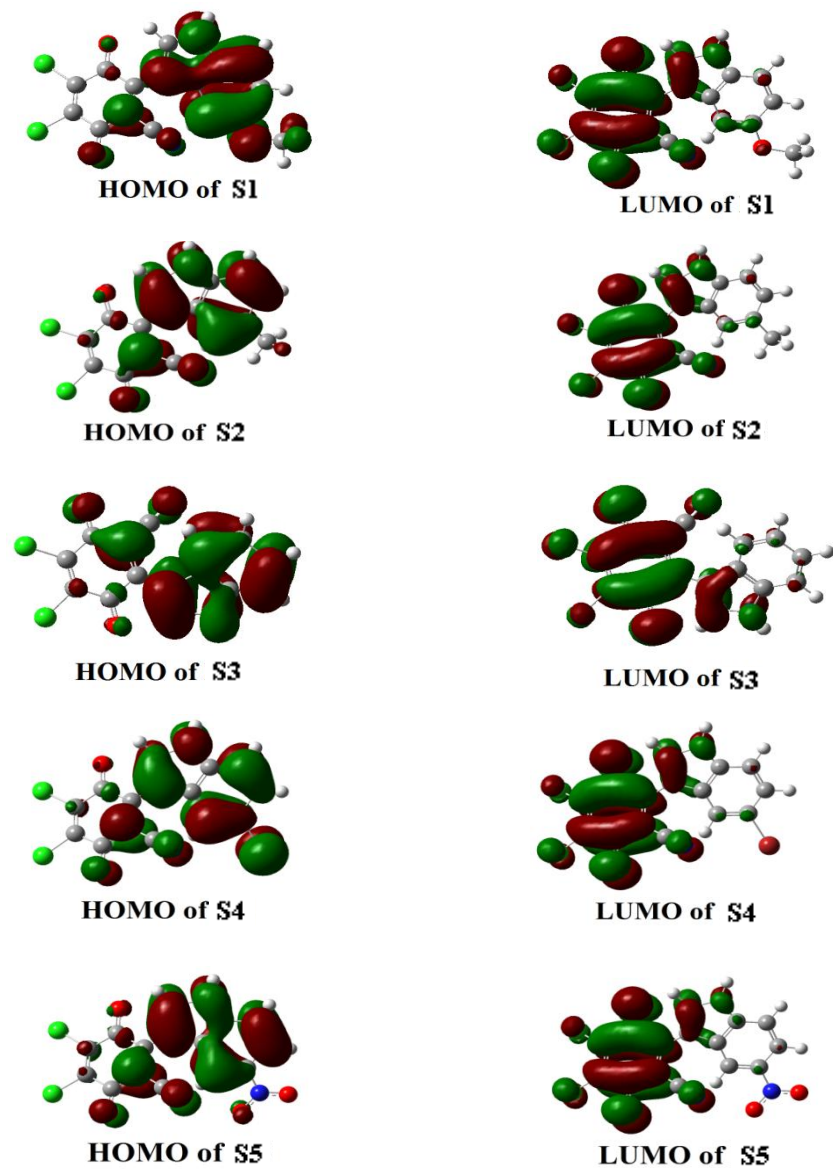


Fig. S33. Molecular orbitals (HOMO–LUMO) of sensors **S1–S5**.

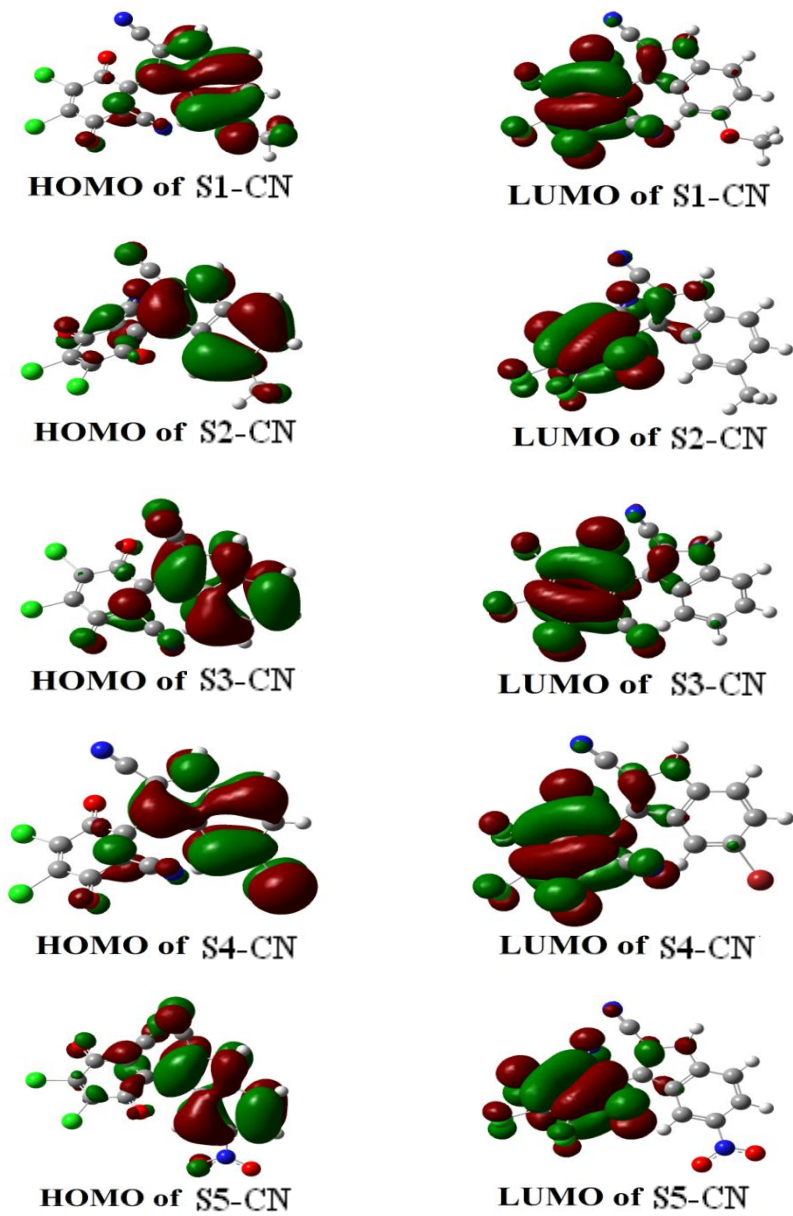


Fig. S34. Molecular orbitals (HOMO –LUMO) of sensors–CN[–] complexes.

Table S1. Energies (in eV) of the MOs in free sensors and in sensor- CN⁻ ion complexes.

Sensor	Free sensor			Sensor-anion complex			$\Delta_{\Delta E}$
	E _{HOMO}	E _{LUMO}	ΔE	E _{HOMO}	E _{LUMO}	ΔE	
S1	-6.2562	-4.3756	1.8806	-6.5452	-4.7027	1.8425	0.0381
S2	-6.5226	-4.4371	2.0855	-6.8682	-4.8184	2.0498	0.0357
S3	-6.5898	-4.4834	2.1064	-6.9876	-4.8175	2.1701	-0.0637
S4	-6.7849	-4.6129	2.1720	-7.1398	-4.9280	2.2118	-0.0398
S5	-7.1738	-4.8331	2.3407	-7.5896	-5.1550	2.4346	-0.0939

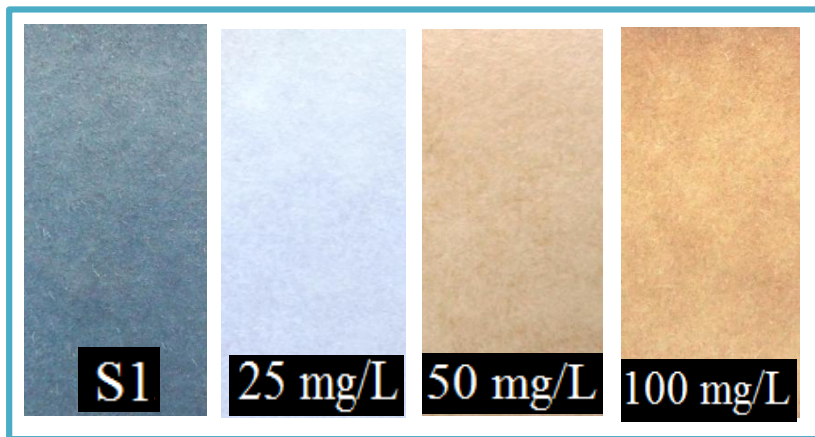


Fig. S35. Color change of test strips upon dipping in solution of NaCN in deep well water.

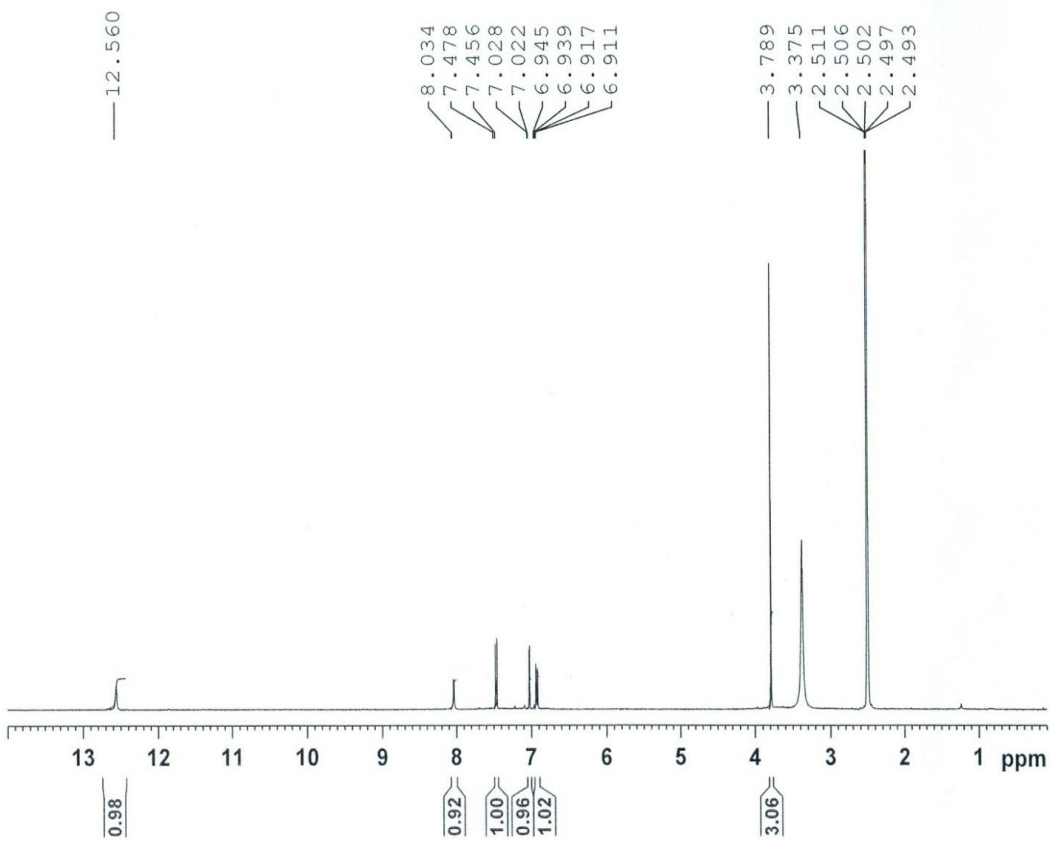


Fig. S36. ^1H NMR spectrum of **S1** in DMSO-d_6 .

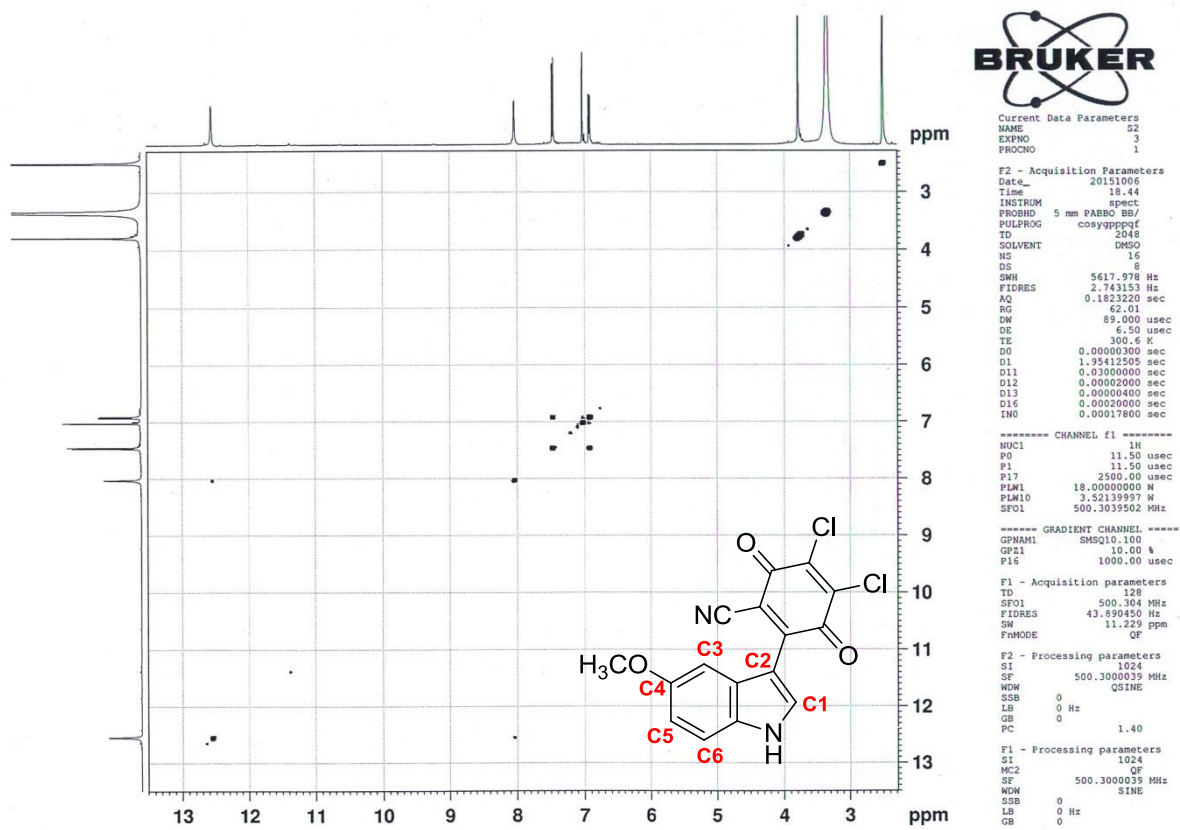


Fig. S37. ^1H - ^1H COSY spectrum of **S1** in DMSO-d_6 .

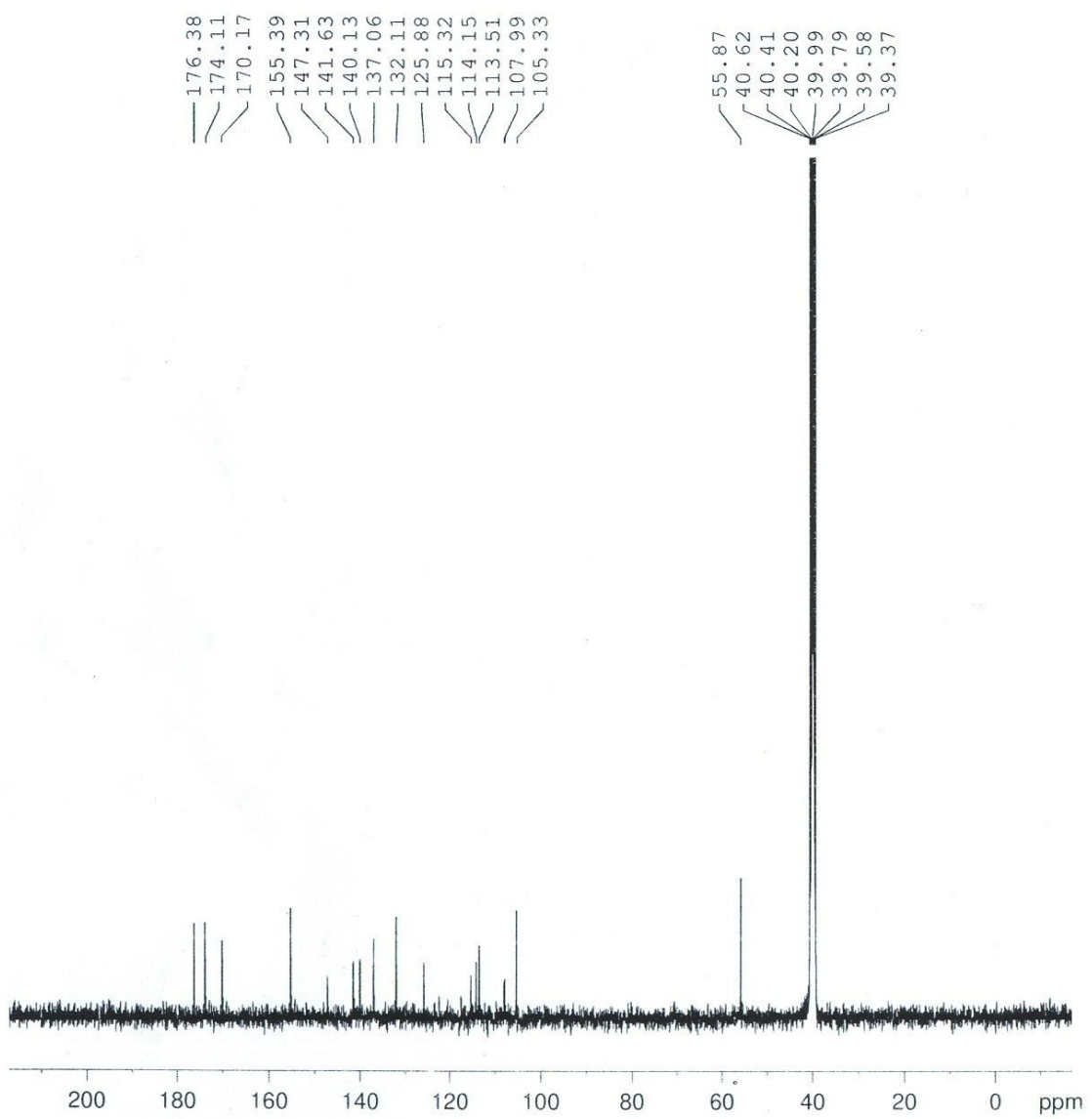


Fig. S38. ^{13}C NMR spectrum of **S1** in DMSO-d_6 .

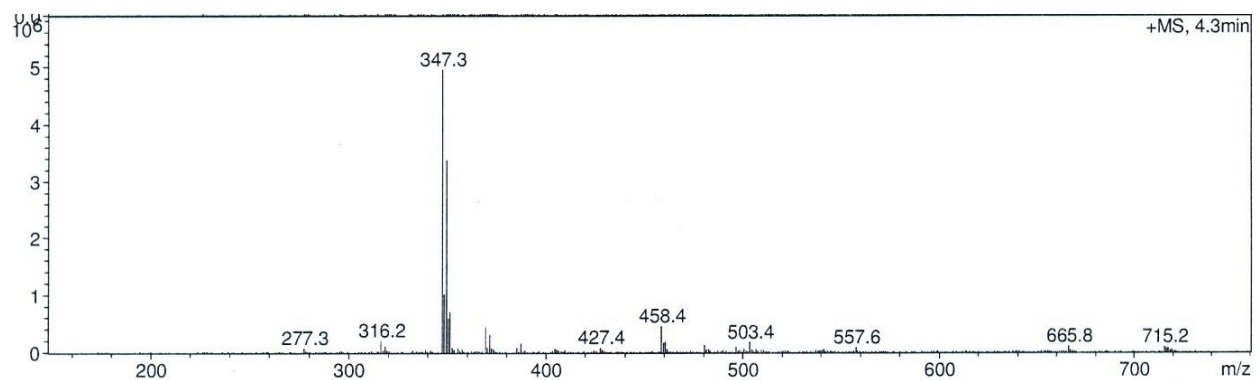


Fig. S39. LCMS spectrum of **S1**.

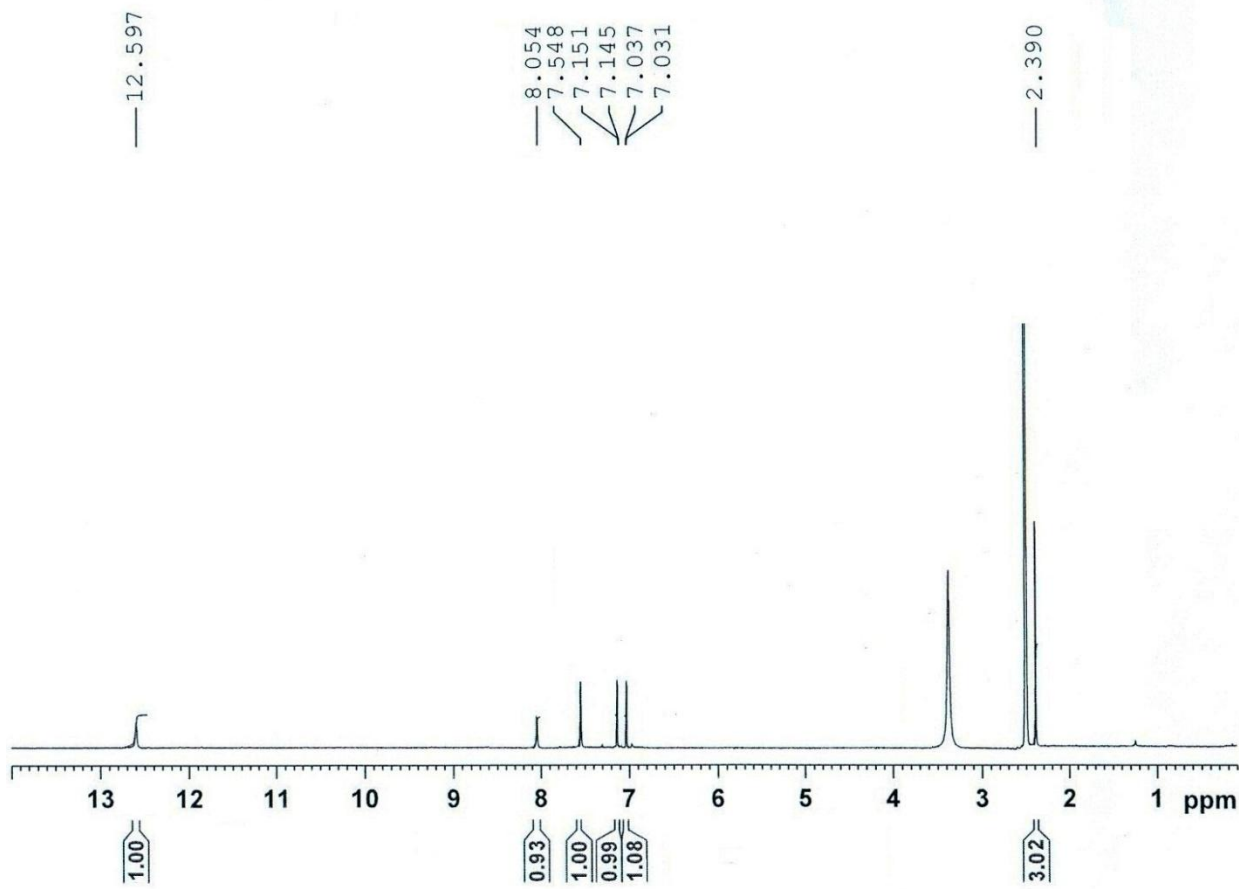


Fig. S40. ^1H NMR spectrum of **S2** in DMSO-d_6 .

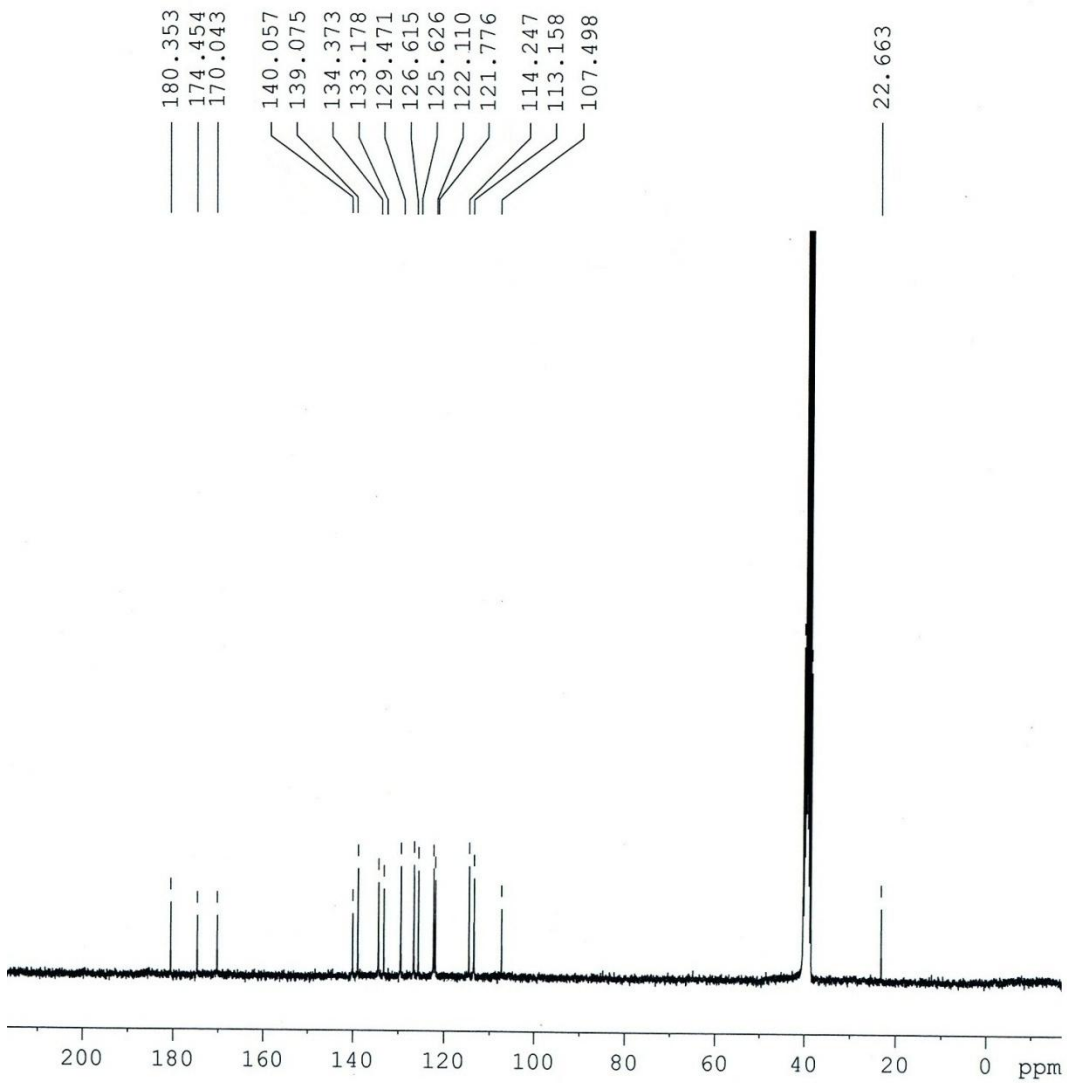


Fig. S41. ^{13}C NMR spectrum of **S2** in DMSO-d_6 .

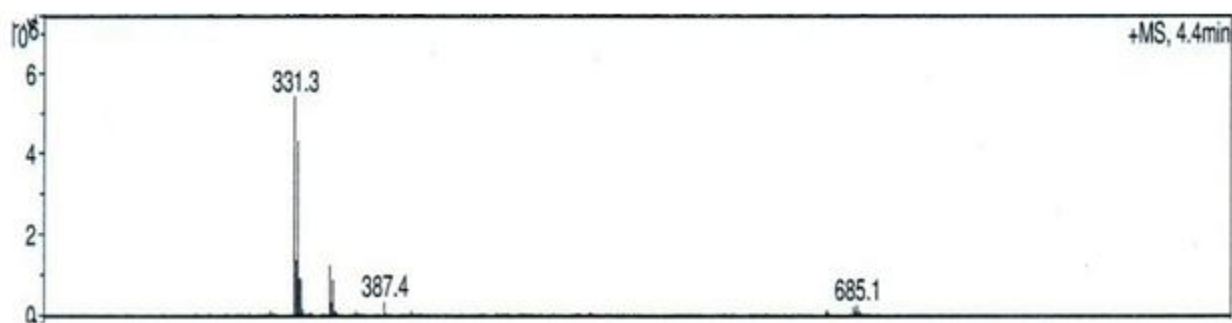


Fig. S42. LCMS spectrum of **S2**.

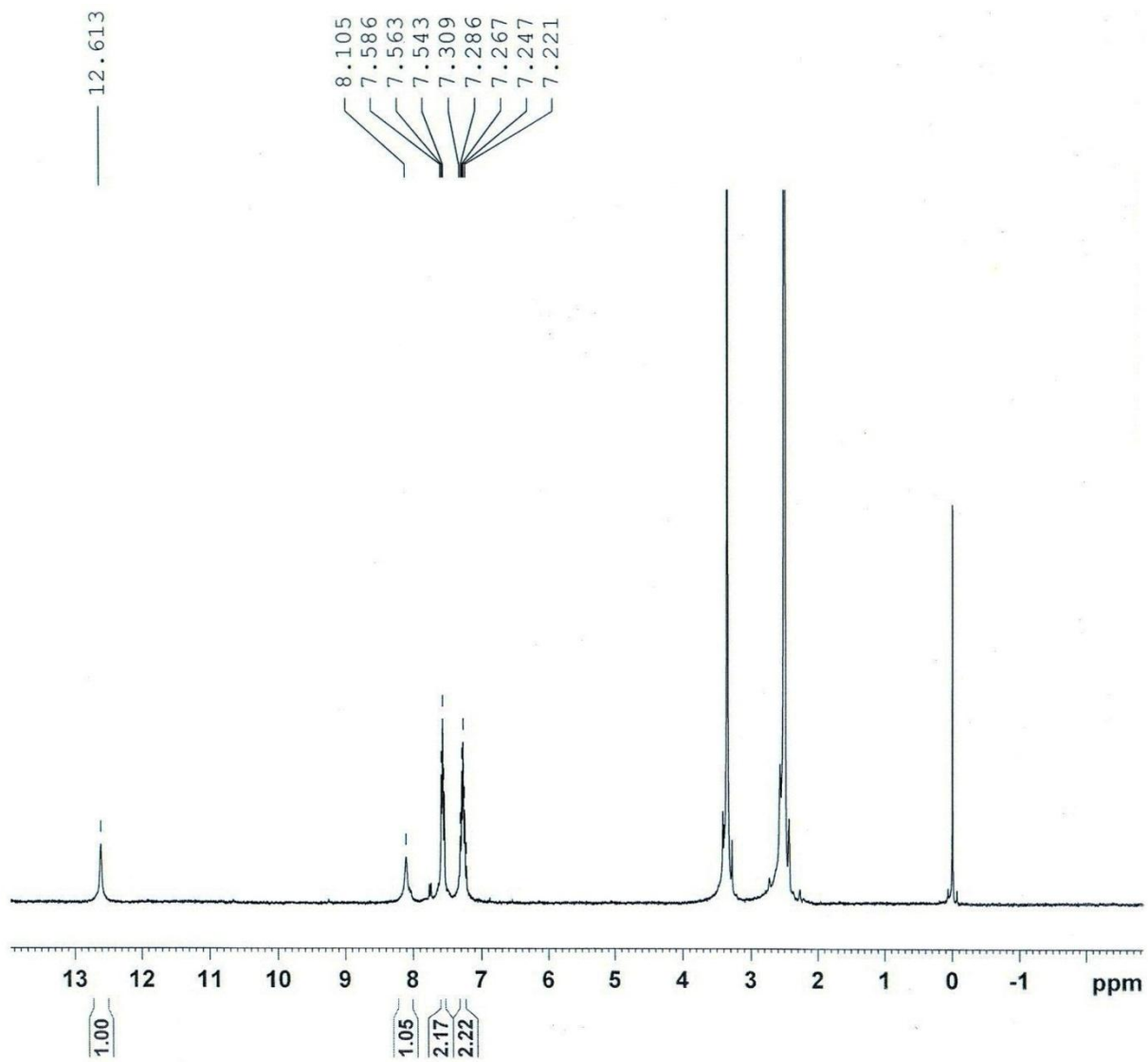


Fig. S43. ^1H NMR spectrum of **S3** in DMSO-d_6 .

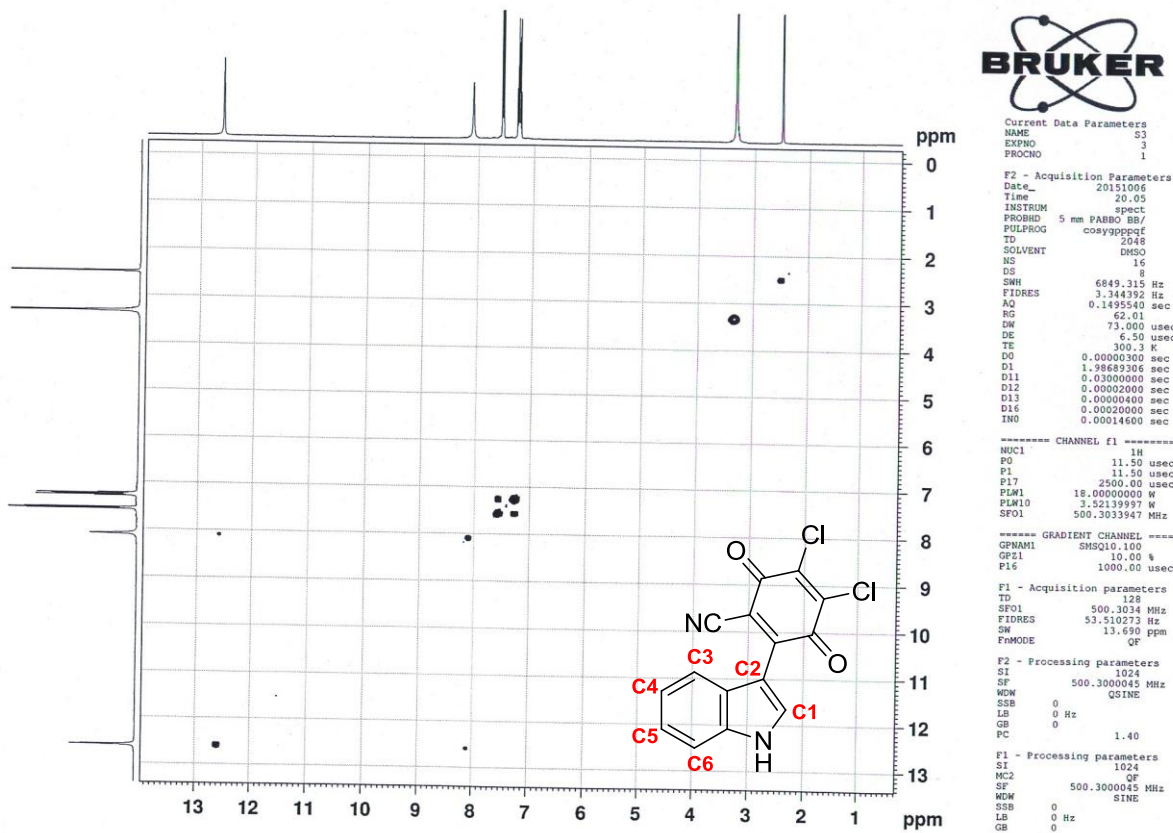


Fig. S44. ^1H - ^1H COSY spectrum of **S3** in DMSO-d_6 .

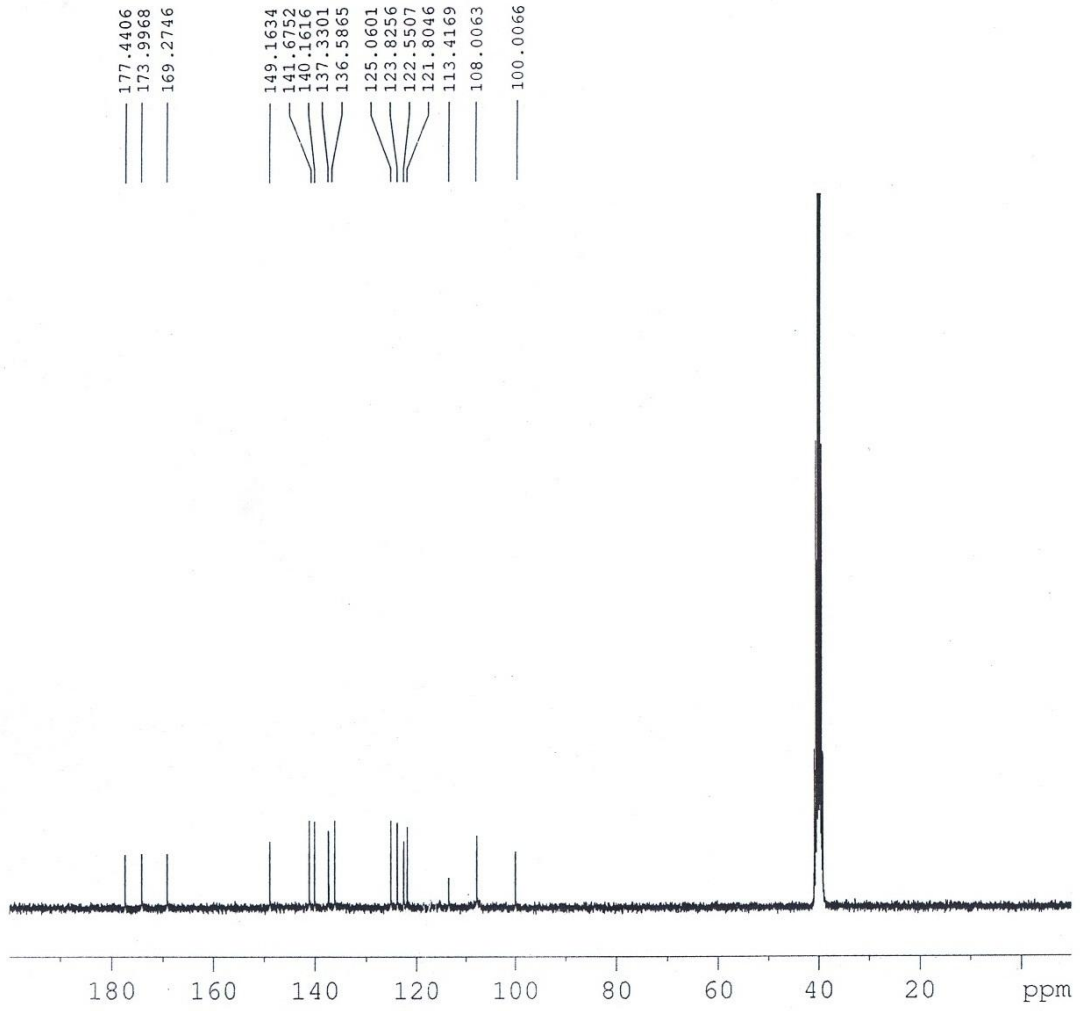


Fig. S45. ^{13}C NMR spectrum of **S3** in DMSO-d_6 .

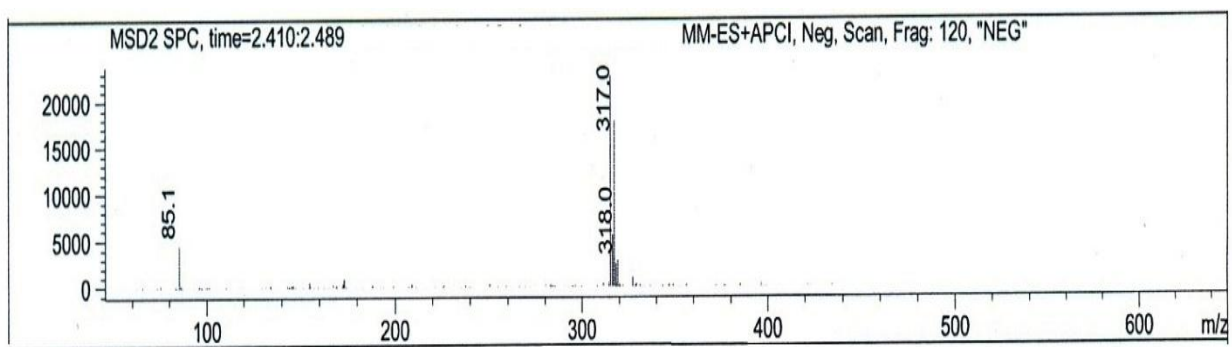


Fig. S46. LCMS spectrum of S3.

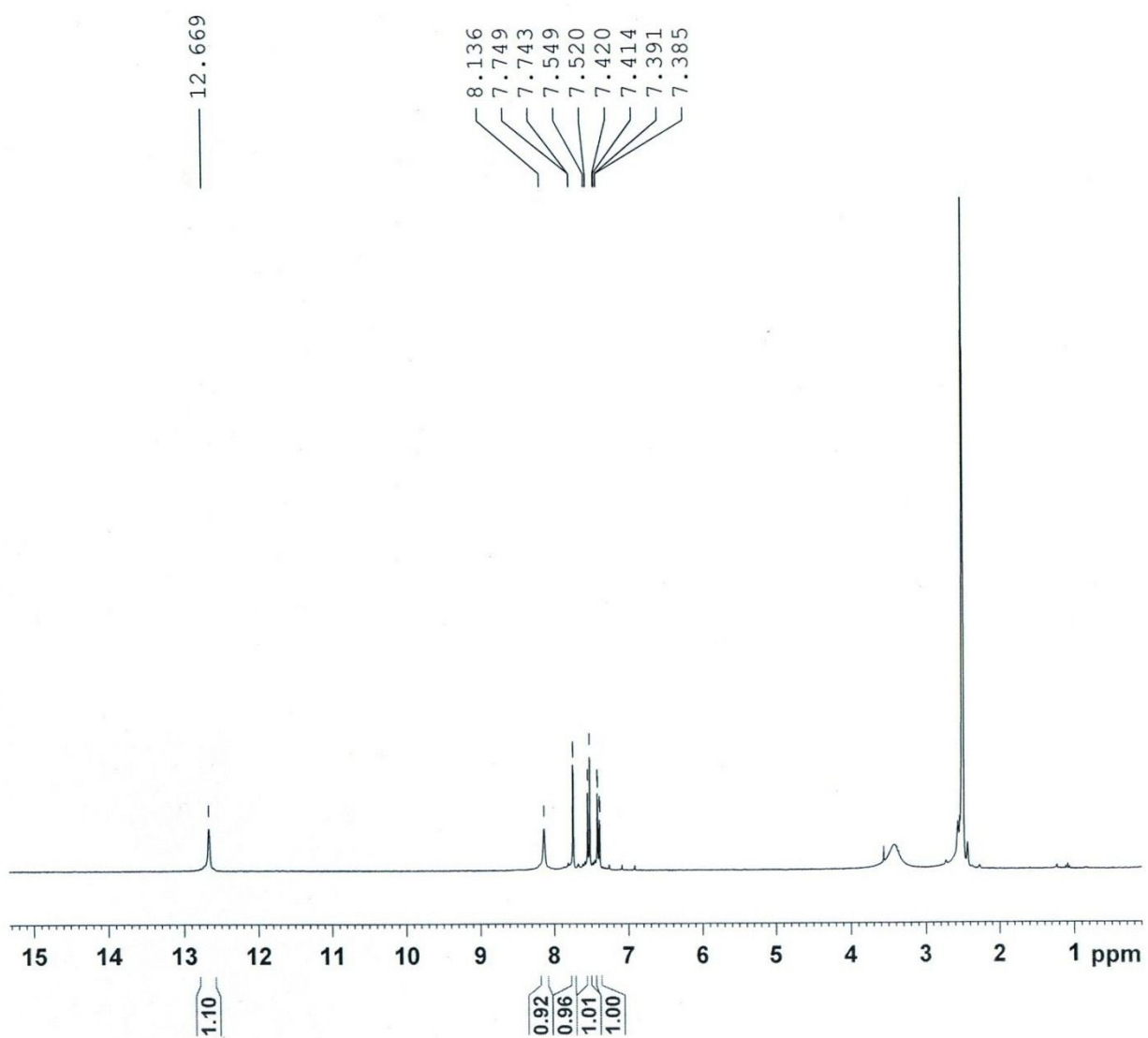


Fig. S47. ^1H NMR spectrum of **S4** in DMSO-d_6 .

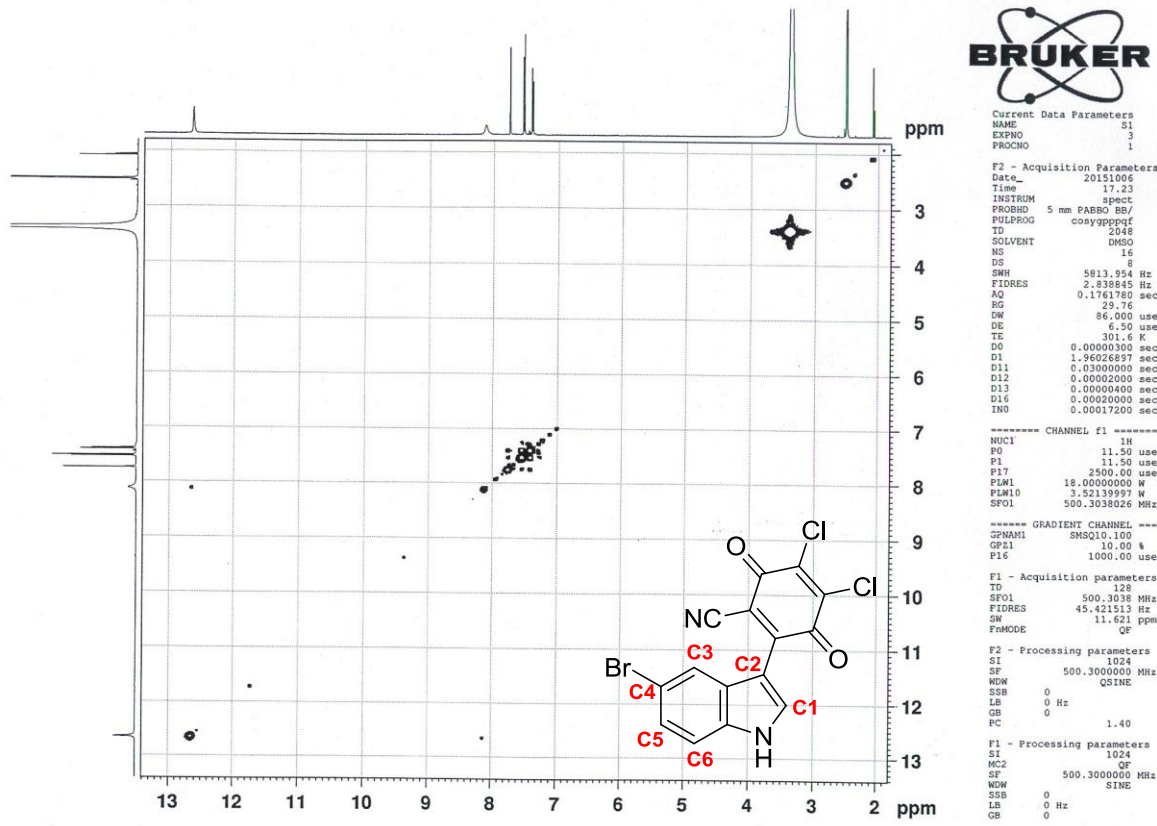


Fig. S48. ^1H - ^1H COSY spectrum of **S4** in DMSO-d_6 .

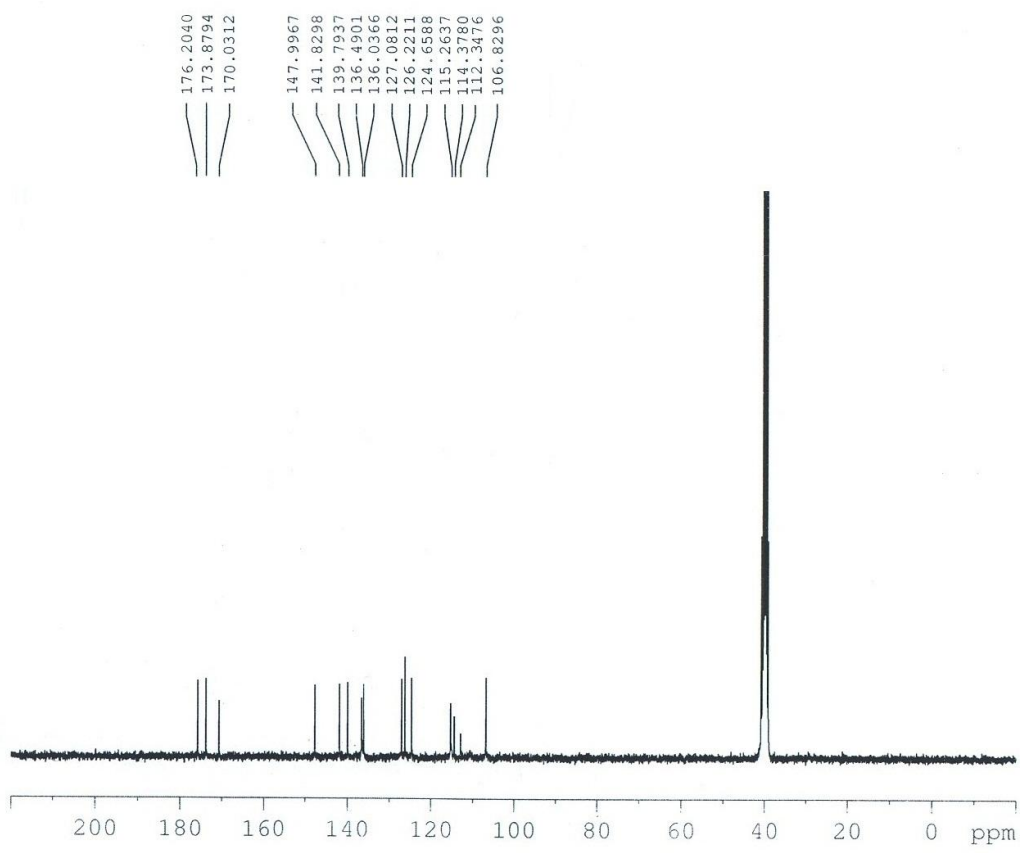


Fig. S49. ^{13}C NMR spectrum of **S4** in DMSO-d_6 .

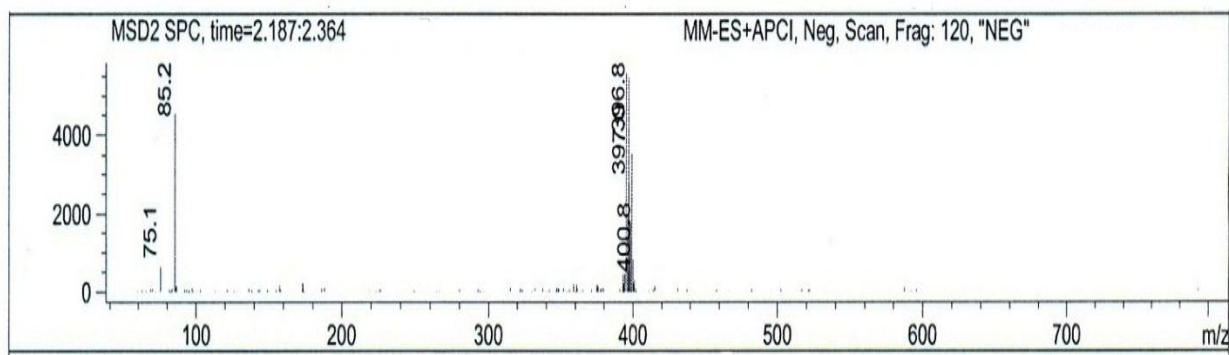


Fig. S50. LCMS spectrum of S4.

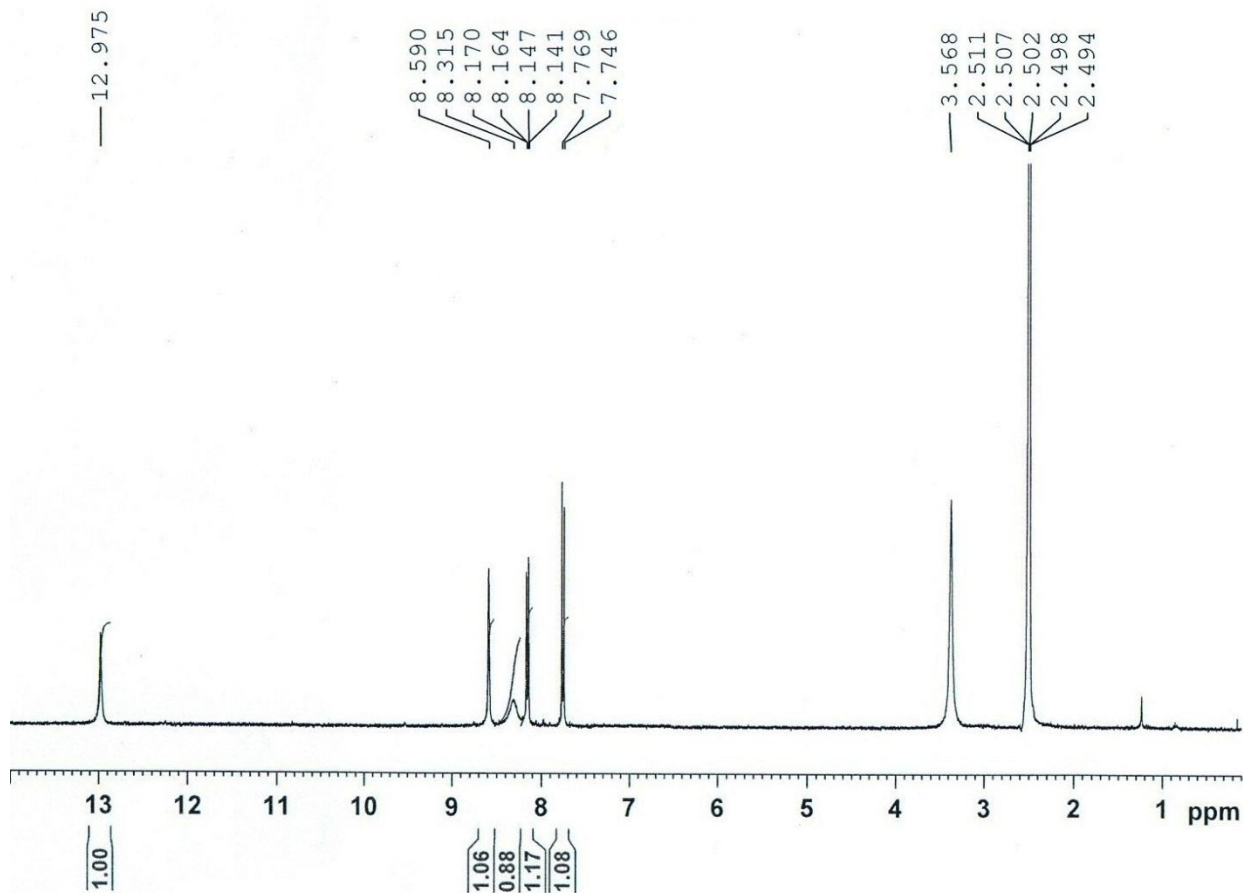


Fig. S51. ^1H NMR spectrum of **S5** in DMSO-d_6 .

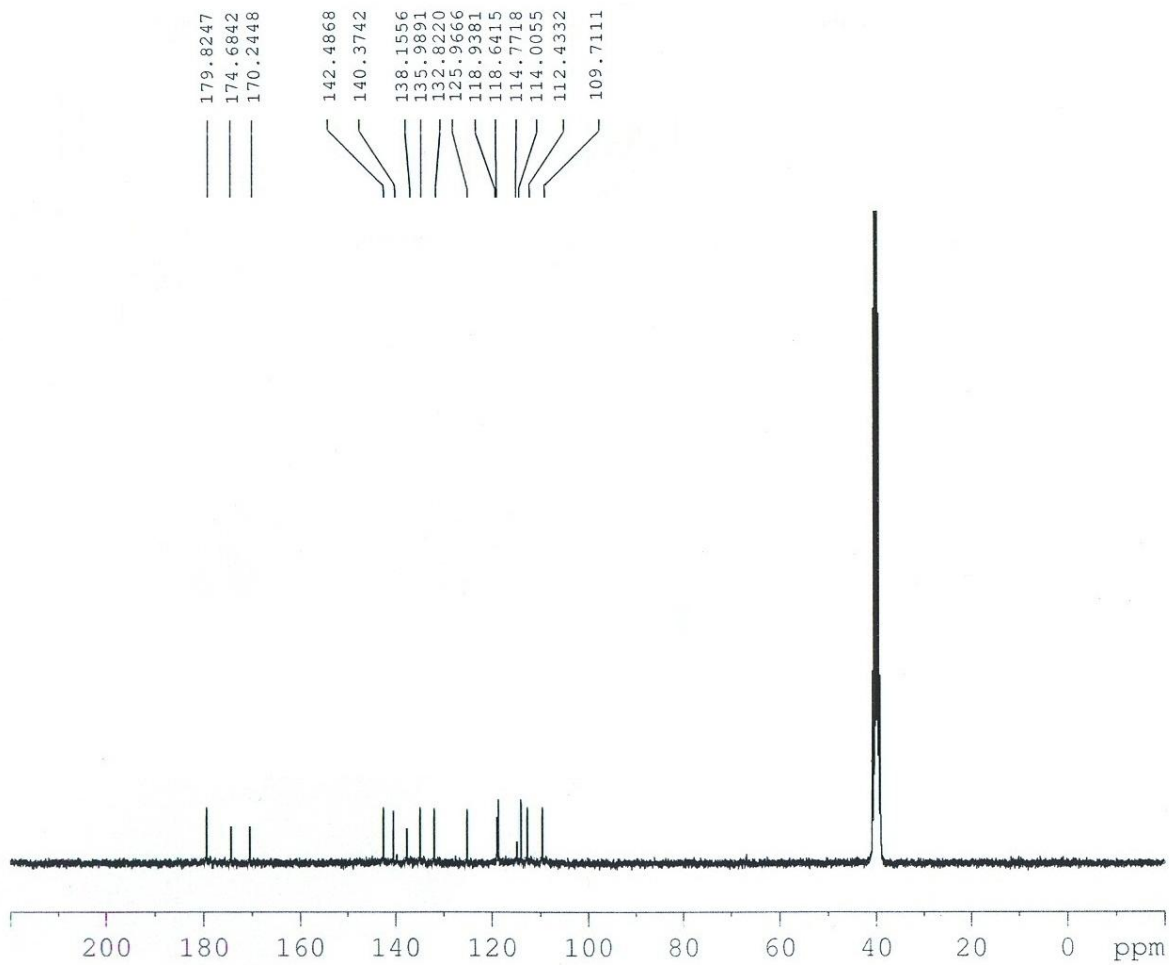


Fig. S52. ¹³C NMR spectrum of **S5** in DMSO-d₆.

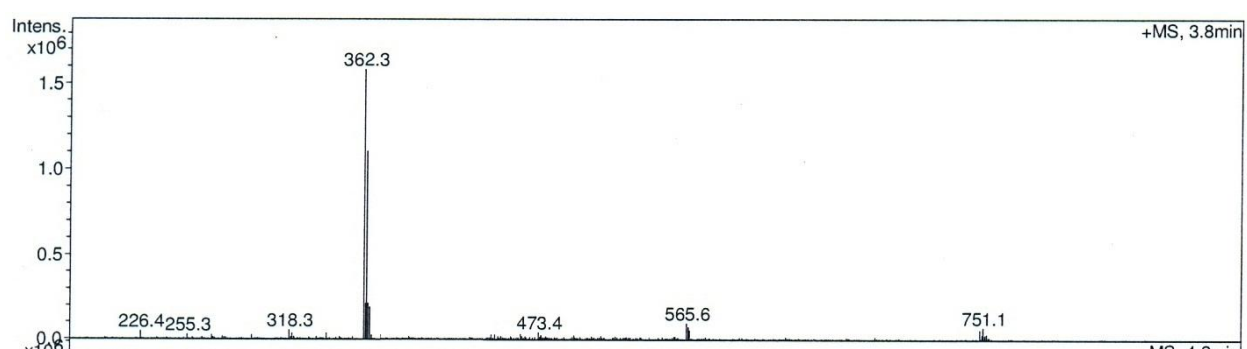


Fig. S53. LCMS spectrum of S5.

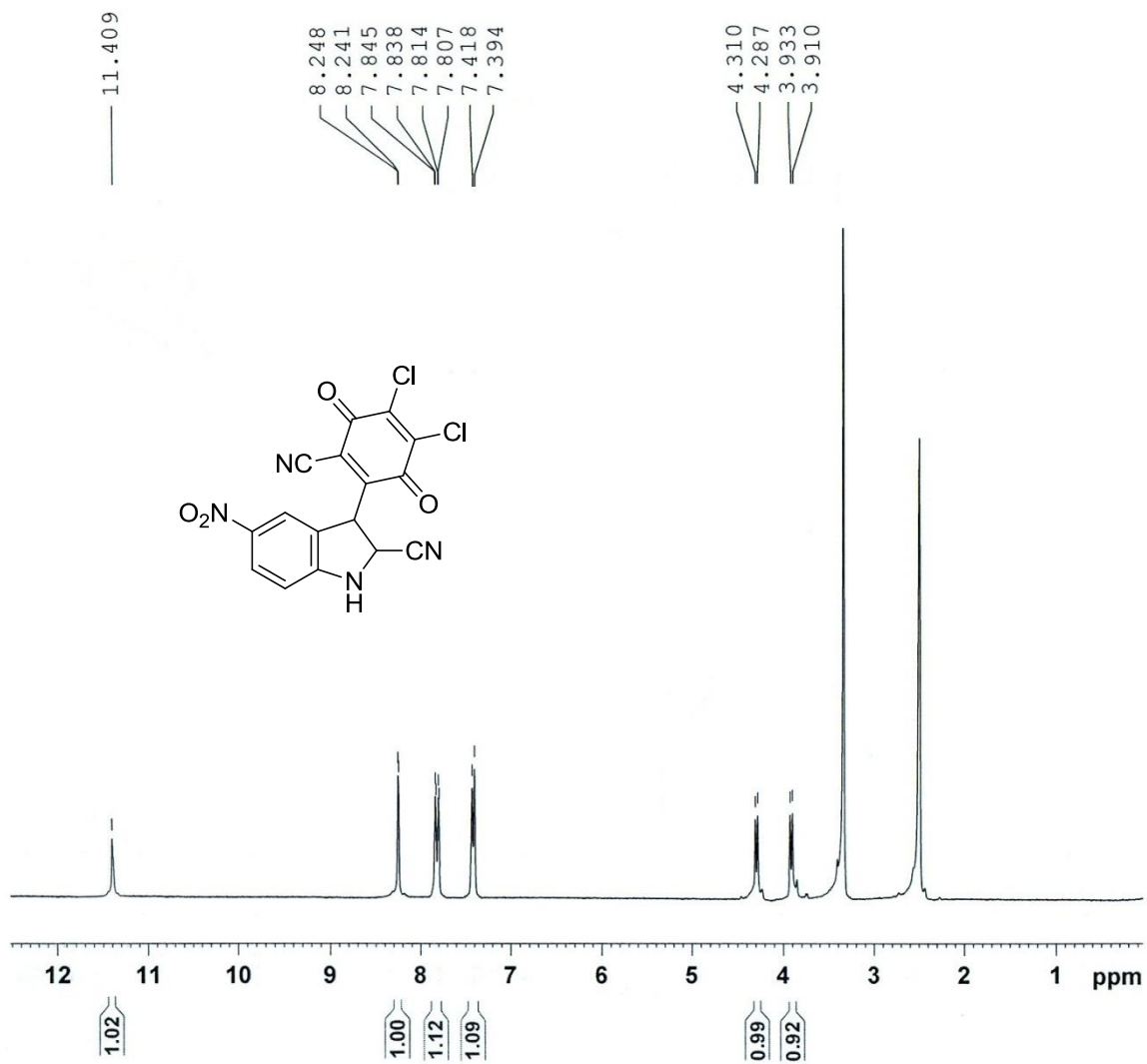


Fig. S54. ^1H NMR spectrum of S5 in DMSO-d_6 .

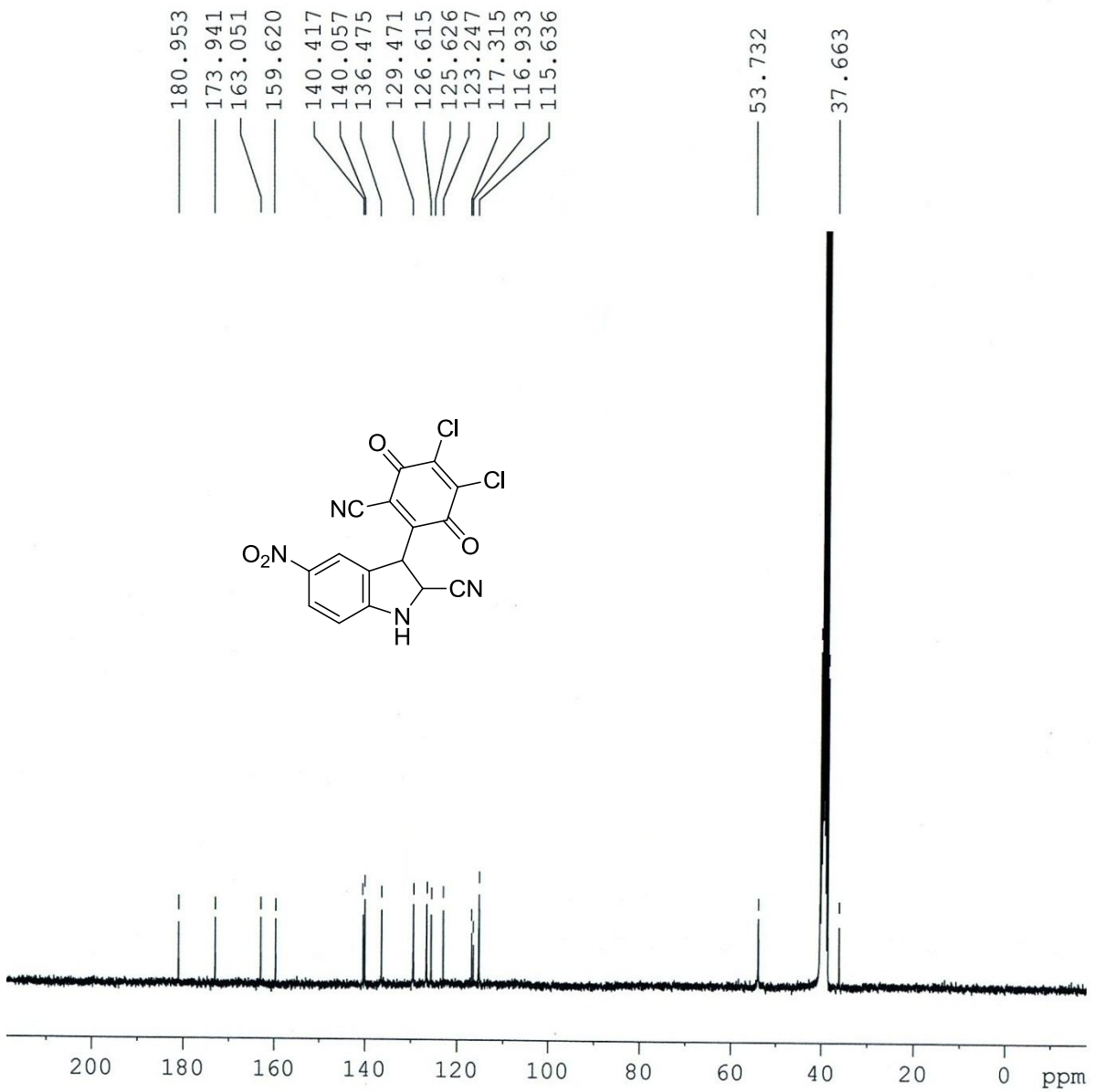


Fig. S55. ^{13}C NMR spectrum of **S5** in DMSO-d_6 .

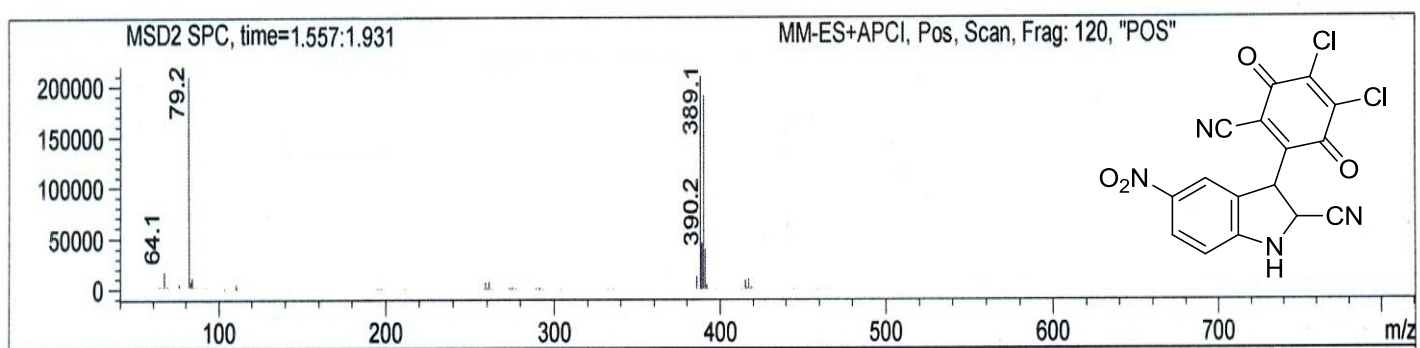


Fig. S56. LCMS spectrum of S5.